



**The Design of a Collimator Mechanism for the Small Angle Mode
K600 Magnetic Spectrometer.**

by

Mulalo Raphalalani

Thesis submitted in fulfilment of the requirements for the degree

Master of Engineering: Mechanical Engineering

in the Faculty of Engineering

at the Cape Peninsula University of Technology

Supervisor: Dr O. Nemraoui

Bellville

November 2019

DECLARATION

I, Mulalo Raphalalani, declare that the contents of this dissertation/thesis represent my own unaided work, and that the dissertation/thesis has not previously been submitted for academic examination towards any qualification. Furthermore, it represents my own opinions and not necessarily those of the Cape Peninsula University of Technology.

Signed

Date

ABSTRACT

The K600 (K is the kinematic factor) magnetic spectrometer at iThemba Laboratory for Accelerator Based Sciences (LABS) is a high resolution detector system, and is one of the kind in the southern hemisphere, first commissioned at iThemba LABS (then known as the National Accelerator Centre) in October 1991. The collimator of the K600 magnetic spectrometer defines the angular acceptance of reaction particles to be detected by the focal plane detection package of the spectrometer. For reaction measurements in the angular range of 6° - 70° , the original collimator carousel with its six possible collimator positions works fine. However, the requirement to have the beamstop right next to the collimator in the small angle mode (to measure the 2° - 6° angular range) cannot be achieved by the use of carousel system. Small angle measurements require that a beamstop be positioned right next to the collimator and with the carousel it is not possible to perform such measurements because the carousel structure does not provide an internal beamstop position. To access the 2° - 6° angular range, the K600 has to be positioned at 4° since the spectrometer has a $\pm 2^{\circ}$ angular acceptance. For measurements at 4° a prototype small-angle mode vacuum chamber was used to connect the K600 to the scattering chamber. The problem with the carousel and the small angle mode was that, it required manual changing of collimators which caused loss of beamtime, and also posed a health risk to staff. The new design is remotely controllable from the data room, which protects employees from being exposed to high radiation level from manually operating the prototype when changing collimator position. The chamber was tested for any deformation through simulation software during the design stage and also during prototype installation to see if it is able to withstand the applied load. To remotely control the prototype, linear pneumatic motor was used coupled with electronics controls to ensure that the operator is able to get accurate positioning of collimator onto the beam line during experimental procedures. Linear potentiometer was used to lock position and also limit switches were utilised to avoid overshooting during positioning process. Air control valve was used to control the flow to the pneumatic motor. The manufactured mechanism was assembled and tested for vacuum and control systems. After installation of the prototype in the K600 vault, (with all the electrical and electronics components required) EPICS software codes were developed and tested at the K600 for remotely control.

Keywords: Collimator, K600 magnetic spectrometer, simulation

ACKNOWLEDGEMENTS

First and foremost, I would like to thank my heavenly father for giving me strength, wisdom and power throughout my studies.

To my supervisor Dr O. Nemraoui, thank you for your time, guidance and support throughout the study. I would like to appreciate my supervisors at iThemba LABS Dr K.V. Mjali and Mr Z Dyers for their guidance, encouragement and help throughout the design and manufacturing process. Your assistance is highly appreciated.

The iThemba LABS (NRF) Facility is acknowledged for providing a facility to carry out the research and their financial assisted is acknowledged.

Ndi tama u livhuwa mmeanga Vho-Florah Mboneni Managa uri vhonyalusa vha ntendela uri ndi tevhele miloro yanga ndi funzee uswika hafha hune ndavha hone namusi, Ndi a livhuwa mme a Mulalo.

To my siblings, Ndivhuwo, Shonisani, Winnie and Takalani, thank you for the encouragement, the selfless love, the support and motivation you gave me throughout the study. Special thanks to my late grandmother. Ndi a vhalivhuwa lufuno lwavho na pfunzo dzevha ntsia nazwo.

Table of content

DECLARATION	ii
ABSTRACT	iii
ACKNOWLEDGEMENTS	iv
LIST OF FIGURES.....	vii
LIST OF TABLES	ix
GLOSSARY.....	x
CHAPTER 1	1
INTRODUCTION.....	1
1.1 Introduction to the facility	1
1.2 Motivation of study.....	1
1.3 Literature review.....	2
1.4 Aim of the Research Project.....	4
1.5 Significance of the study	4
1.6 Research Methodology	5
1.7 Expected Outcomes	6
1.8 Delineation of the Research.....	6
1.9 Chapter Overview	6
CHAPTER 2.....	7
Design overview	7
2.1 Collimator.....	7
2.2 Beamstop configuration.....	8
2.3 Collimator holder	12
2.4 Model design.....	13
2.5 Positioning system	13
CHAPTER 3	19
Modelling and Simulation Study.....	19

3.1 Introduction	19
3.2 Design simulation software	19
CHAPTER 4	23
Simulation results and discussion	23
4.1 Simulation results.....	23
4.2 Conclusion for this chapter	39
CHAPTER 5	40
Assembly and installation of the model, Testing and validation	40
5.1 Assembly of the motor drive mechanism:	41
5.2 Chamber assembly	42
5.4 Control systems.....	43
5.3 Test and Validation	47
CHAPTER 6	49
Conclusions and Recommendations.....	49
6.1 Conclusions	49
6.2 Recommendations	50
BIBLIOGRAPHY	51
APPENDICES.....	54
APPENDIX A.....	55
Detailed drawings of the three collimators	55
APPENDIX B.....	61
Overall detailed design of the prototype	61
APPENDIX C	64
Epics Substitution file.....	64
Epics IOC data base template	67
Epics IOC execution template	71

LIST OF FIGURES

Figure 1.1: K600 magnetic spectrometer overview schematic (Adsley et al., 2017).	2
Figure 2.1: The peperpot collimator with insert.....	7
Figure 2.2: Beamstop with clear flange.	9
Figure 2.3: First scattering chamber in the middle 1990's.	10
Figure 2.4: The scattering chamber used from 1999.	10
Figure 2.5: The cake scattering chamber during its commissioning run in 2014.	11
Figure 2.6: The sliding seal scattering chamber in 2015.....	12
Figure 2.7: Collimator holder.	13
Figure 2.8: Motor dimensions (Langro, 2011).	16
Figure 2.9: Schematic of the 5/3 – way valve (Festo, 2018).	16
Figure 2.10: Automated pressure control with solenoid alternatives. (Womack, 1990).	17
Figure 2.11: Linear potentiometer (Festo, 2018).	18
Figure 2.12: EL2808 – Linear Solenoid Switch (Rs components, 2018).	18
Figure 3.1: FEM process.....	20
Figure 3.2: Buckling beam.	21
Figure 3.3: Stress strain curve to analyse material properties (Philipfigari, 2015).	22
Figure 4.1: Camber body.	24
Figure 4.2: Chamber displacement.	27
Figure 4.3: Stress results.	28
Figure 4.4: Factor of safety results.	29
Figure 4.5: Eigenvalue buckling results.	31
Figure 4.6: Drive assembly.....	33

Figure 4.7: Displacement results of the motor drive.....	36
Figure 4.8: Stress results of the drive.....	37
Figure 4.9: Factor of safety results.....	38
Figure 5.1: Prototype assembly.....	40
Figure 5.2: Motor drive.....	41
Figure 5.3: Chamber body.....	42
Figure 5.4: Control system flowchart.....	44
Figure 5.5: Collimator positioning.....	45
Figure 5.6: Chamber leak testing.....	47
Figure A.1: Solid collimator.....	55
Figure A.2: Collimator accommodating inserts.....	56
Figure A.3: Peperpot insert.....	57
Figure A.4: Angular insert.....	58
Figure A.5: Collimator with peperpot insert assembly.....	59
Figure A.6: Three collimators assembled to the ladder.....	60
Figure B.1: Chamber assembly.....	61
Figure B.2: Top level assembly driving the motor.....	62
Figure B.3: The prototype assembled with the sliding seal scattering chamber.....	63

LIST OF TABLES

Table 2.1: Motor specifications.....	15
Table 2.2: Valve Specifications.	17
Table 4.1: Characteristics of Chamber's parts.....	25
Table 4.2: Properties of stainless steel 316L from Solid Edge data base.	25
Table 4.3: Chambers displacement results.	27
Table 4.4: Chambers stress results.....	28
Table 4.5: Chambers factor of safety results.	29
Table 4.6: Buckling results.	30
Table 4.7: Characteristics of drive assembly parts.	34
Table 4.8: Properties of Aluminium and Stainless Steel from Solid Edge database.....	35
Table 4.9: Displacement results of motor drive assembly from Solid Edge.....	36
Table 4.10: Stress results of the drive from Solid Edge.	37
Table 4.11: Factor of safety results from Solid Edge.	38

GLOSSARY

Abbreviations/ Acronyms	Definition/Explanation
LABS	Laboratory for Accelerator Based Sciences
K600	Kinematic factor
°	Degree
SSC	Separated-sector cyclotron
CAD	Computer-aided design
EPICS	Experimental Physics and Industrial Control System
FEA	Finite element analysis
POT	Linear potentiometer

CHAPTER 1

INTRODUCTION

1.1 Introduction to the facility

iThemba laboratory for accelerator based sciences (LABS) is a multidisciplinary facility which provides basic and applied research, proton and neutron radiotherapy for cancer treatment and supplies radionuclides for use in the nuclear medicine and research (Kheswa et al., 2008). There are several vaults at the facility such as experimental vaults, radiotherapy vaults, isotope production vaults and more. They all get their beam of particles from the separated-sector cyclotron (SSC). The SSC is capable of accelerating protons to energies of 200 MeV and can accelerate heavier particles to energies between 30 and 40 MeV per nucleon.

The subatomic physics department consist of three active vaults namely, the K600 magnetic spectrometer, the Afrodite gamma-ray detector array. This study is going to focus on the K600 magnetic spectrometer. The K600 magnetic spectrometer is used to study light charged particles emitted in nuclear reactions. The current study aims at improving the collimator mechanism for the small angle mode of the K600 magnetic spectrometer in order to accommodate all angle mode of the spectrometer.

1.2 Motivation of study

The collimator of the K600 magnetic spectrometer defines the angular acceptance of reaction particles to be detected by the focal plane detection package of the spectrometer (Neveling et al., 2008). For reaction measurements in the angular range 6° - 70° the existing carousel system with six possible collimator positions works well. However, the requirement to have the beamstop right next to the collimator in the small angle mode (to measure the 2° - 6° angular range) means that this carousel system cannot be used for the K600 positioned at 4° .

The problem with the current setup is that there are two different prototypes that need to be manually changed for specific angles and these manual changes pose health risk to staff who will be handling the system after it had been exposed to high level radiation and also cause loss of beamtime.

1.3 Literature review

1.3.1 Magnetic Spectrometer

The K600 magnetic spectrometer at iThemba LABS is a high resolution detector system and is one of its kind in the southern hemisphere, it was first commissioned at iThemba LABS (then known as the National Accelerator Centre) in October 1991. It is the same as the former K600 magnetic spectrometer at Indiana University Cyclotron in terms of its size and the average flight path for a particle from the target to the detector (Neveling et al., 2017). “K600 transmission mode was originally used to understand and eliminate the beam halo at the target location of the K600 High resolution spectrometer” (Berg et al., 1993-1994).

The spectrometer consists of five active elements namely, a quadrupole which is located at the entrance of the spectrometer, two dipoles bending magnets and two trim coils which are located inside the dipoles (Usman, 2009) as shown in figure 1. The quadrupole at the entrance is used for vertical focusing at the focal plane, while the two dipole magnets are used to separate the mass and momentum, and the two trim coils are used to achieve the final focusing at the focal plane. The K600 magnetic spectrometer is used for measurements of inelastic proton or alpha scattering, as well as transfer reactions at very small angles including 0° (Adsley et al., 2017). The measurements taken at the K600 can be used to solve several problems including the properties of the isoscalar enormous monopole and dipole resonances.

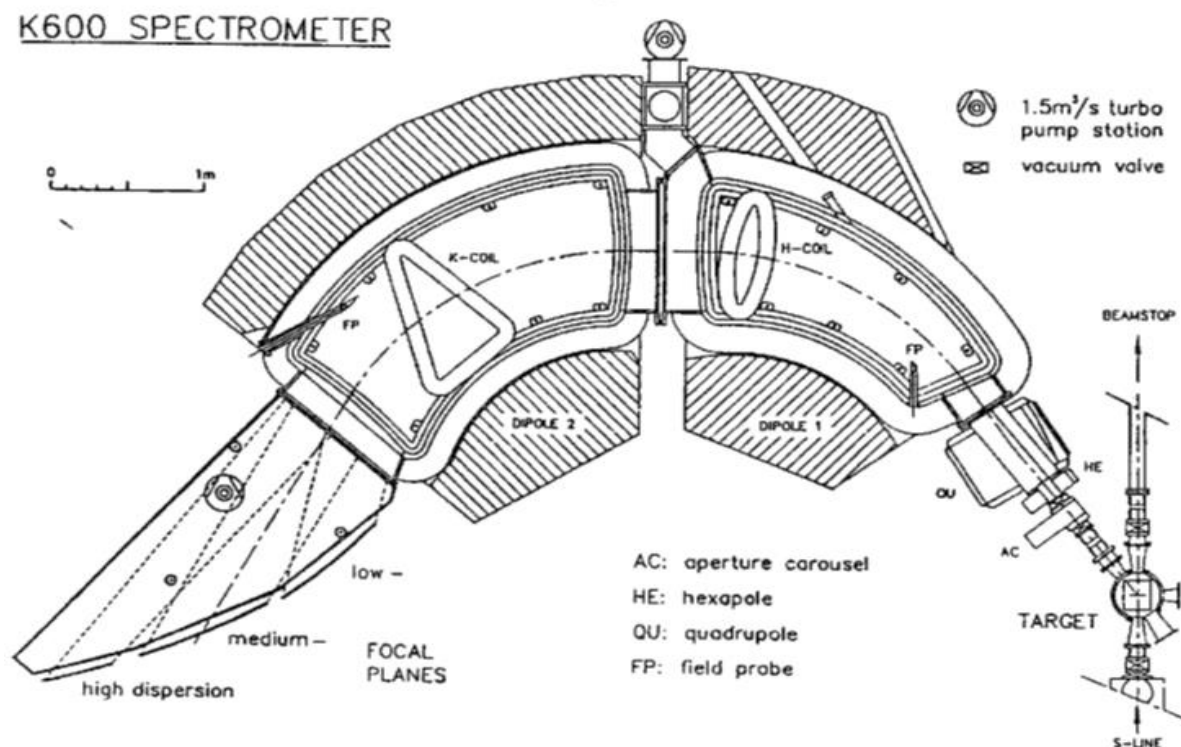


Figure 1.1: K600 magnetic spectrometer overview schematic (Adsley et al., 2017).

1.3.2 Design Simulation

Simulation of the manufacturing processes or predicting of the manufacturing methods used to make the product is commonly referred to as virtual manufacturing (Shailendra, Prakash & Vivek, 2015: 350). It helps designers to design for manufacturability and manufacturing efficiency. It is important for a designer to always start every design with the manufacturing process in mind as it helps save money and time, rather than to change drawings after they had being sent out for manufacturing process. With simulation model, the designer gets more flexibility in the model development process compared to physical prototype testing. Design simulation can provide more types of analysis results that might be impossible to obtain through physical testing due to practical reasons. With physical prototype there are lots of challenges that a designer can encounter i.e. time required to build physical prototype might delay the project, performance of prototype not matching final product performance, etc. Some of the benefits of design simulation include reducing time waste by avoiding repeated physical prototype testing, and improving quality, also it can help improve the design. The design simulation can include varied analyses that basically test performance of a model under various operating conditions. In this study the simulation focuses on the operating condition as the prototype is required to be able to withstand the radiation level in the vault. The material to be used inside the chamber need to be able to accommodate charged particles so their selection was based on that requirements.

1.3.3 Collimator

Collimator is a device used to control the direction of the beam of particles or waves (Wronka, 2011). It is the first processing layer of a gamma camera to encounter photons from radioactive source. Collimators restrict the rays from the source so that each point in the image corresponds to a unique point in the source. It consists of five basic designs to channel photons of different energies to magnify or minify images, and to select between imaging quality and imaging speed (Shiraza et al., 2013: 278). According to de Vasconcelos et al (2011) the resolution and efficiency of the radiation are the main things to consider when improving the design of industrial collimators. At the radiation profile, resolution is mostly defined as the full width at half-maximum (FWHM) radiation from the source projected by the collimator to the detector. The distance from the source to the collimator and diameter of the collimator are mainly considered in calculating the resolution (Sorenson & Phelps, 1987). The fraction of gamma rays passing through the collimator per gamma rays emitted by source towards the collimator is known as the efficiency.

1.4 Aim of the Research Project

The project aims to provide an improved collimator mechanism for the K600 magnetic spectrometer angle mode to fulfil the following requirements:

- Perform all angle mode experiment at the K600,
- Allow the use of beamstop next to the collimator,
- Save beamtime and
- Be remotely controllable.

1.5 Significance of the study

The study investigates the design and manufacturing of the collimator mechanism which accommodates the beam-stop. Once the best design was selected, a remote positioning system suitable for the design was also selected. According to experimental requirement a software program based on epics was developed to remotely control the position of the collimator ladder onto the beam-line.

The advantages of having this software program being the following:

- The system can be controlled from the data room,
- Employees are not exposed to high radiation from manual changes of different models as the study provides a model suitable for all angle experiments of the K600 magnetic spectrometer,
- Less beamtime loss.

The project outcome is a collimator mechanism which is used in the K600 magnetic spectrometer to perform experiments at all angle modes especially 4°. The K600 magnetic spectrometer should be able to do all angle changes without any configuration of the scattering chamber hardware or vacuum breaks.

1.6 Research Methodology

Existing positioning systems used in industries for linear alignment were carefully analysed (investigated) to ensure that a suitable system is selected for the positioning of the collimator ladder onto the beamline. The selection of this positioning system was based on the model weight and the operating conditions (radioactive environment). The model was designed to accommodate 3 collimators on the ladder and to fit on the existing beam line just upstream of a valve that connects to the K600 quadrupole vacuum chamber.

1.6.1 Research Design Tools

Computer-aided design (CAD) software was used for the project design and simulation. Simulation was done on the final design to ensure that the design met the specifications. The Experimental Physics and Industrial Control System (EPICS) software was used by end user (scientists) to communicate with the positioning system (Pneumatic motor) during experiments or experimental setup.

1.6.2 Design Methodology

- Identification and selection of material to be used in a radioactive environment;
- Designing and simulating the loading capacity and mechanical strength of the model using CAD software (Solid Edge);
- Determine the efficient control system for accurate positioning of collimator ladder;
- Designing and building of Small angle beam-stop to accommodate measurements between 2° - 6° ;
- Manufacturing and assembling of the model;
- Install the model at the K600 magnetic spectrometer;
- Testing and validation of the model.

1.7 Expected Outcomes

- The design and manufacturing of a fully functional collimator mechanism with pneumatic drives for remote control;
- The design of collimator inserts using existing and proven designs.
- It should be possible to do reaction measurements safely for all angle modes of the K600 magnetic spectrometer;
- It should be possible to perform measurements at 4°, (meaning that a small angle beam-stop must be part of the design);
- It should be possible to easily remove the brass beam-stop when it is not required;
- It should be possible to do angle changes without any configuration of scattering chamber hardware or vacuum breaks;

1.8 Delineation of the Research

In this project, an in depth study was done on the linear positioning system (pneumatic drive system) of the collimator ladder, as the accuracy required was essential (± 0.2 mm). The beamstop design required for small angle experiments should cater for angles between 2° - 6°. The collimator ladder should be remotely controllable from the data room. The materials used were investigated as the model operates in a radioactive area, meaning it needed to be able to withstand effects of radiation. The positioning system (pneumatic motor with ball screw) uses special seals and valves that can withstand radiation exposure.

1.9 Chapter Overview

Chapter One: Introduction

Chapter Two: Design overview

Chapter Three: Design and Simulation study

Chapter Four: Results and discussion

Chapter Five: Assembly, Installation, Test and Validation

Chapter Six: Conclusions and Recommendation

CHAPTER 2

Design overview

In this chapter the basic design of components are presented. All major components are described with their material selection and the reason why such materials were selected

2.1 Collimator

According to Jordan & Williams (1994: 231-251) “Collimators have been in use for more than 20 years”. During experiments, a collimator is mostly used to shape the beam of particles, to reduce beam spread in order to get good energy resolution, and also to shield or protect the detectors. When the beam interacts with the target inside the scattering chamber, charged particles are emitted, and only particles that go through the collimator opening are able to enter the bending magnet which is then directed to the focal detectors through the bending magnet.

For this study the collimator is made out of brass material and the reason for using brass due to the fact that brass material has a high stopping power, charged particles that do not go through the collimator opening are stopped. There are different types of collimators and inserts being used at the K600 magnetic spectrometer. For this study two different collimators and two inserts were developed. Shown in figure 2.1 is one of the insert developed with collimator holder. Refer to appendix A for the detailed drawing with sizes.

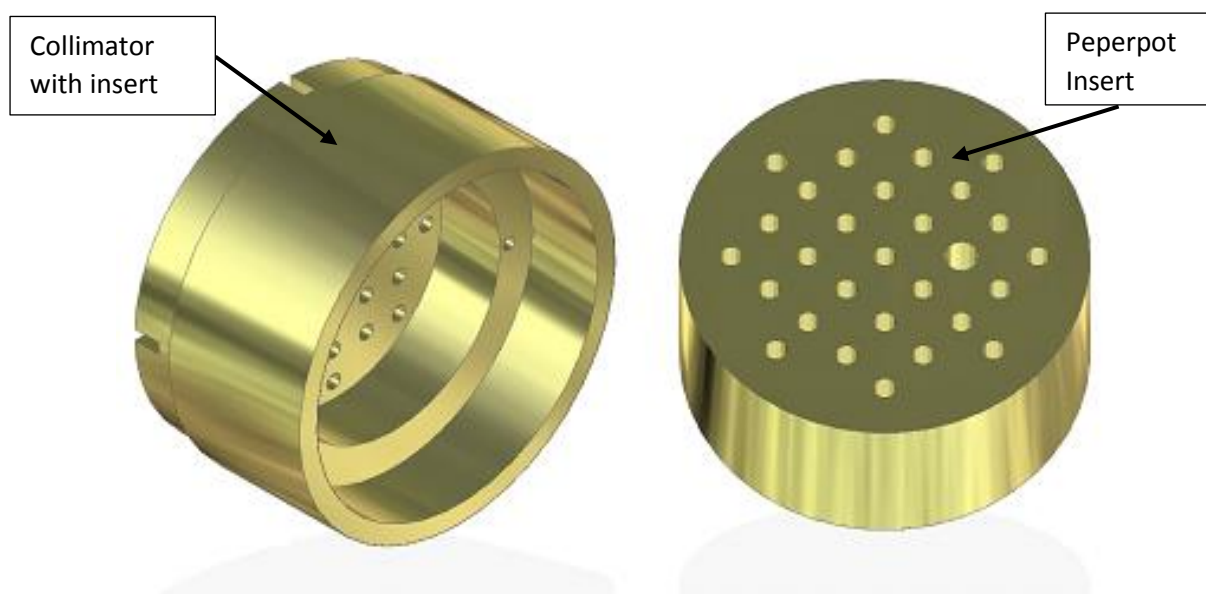


Figure 2.1: The peperpot collimator with insert.

While improving the collimator the main factor to take into consideration is the energy of the particles that needs to be stopped by the solid part of the collimator. The Particle energy depends on the beam energy and high energy particles require higher stopping power, hence the collimator is thick enough to stop them.

2.2 Beamstop configuration

The first beamstop to ever being designed was in the late 90s called Low Energy Demonstration Accelerator (LEDA), it had the ogive shape and was able to absorb 6.7 MeV beam (Van Hagan, et al 1998). For this study the beamstop was manufactured from brass because it has high stopping power, it is cost effective, and the ease of cooling down to avoid overheating.

The beamstop was designed using CAD software (Solid Edge) with dimensions 94.3 X 60 X 38 (mm). While designing the beamstop, the requirement to be able to remove the beamstop when performing an experiment at angles that do not require it was taken into consideration. Hence it is designed in such a way that it can be easily removed when it is not needed. However for it to be easily accessible it was bolted on the clear conflat flange (cf-flange) mounted on the chamber side. The reason for it being clear is to give the operator a point to double check if the collimator is aligned at the beam center, and to be able to have a view on what is happening inside the chamber during experiment preparations.

As seen in the figure 2.2, the beamstop opening is close to the edge in order to accommodate small angles. Two aluminum plates are bolted on the beamstop and are used to hold two small magnets which are required during experiments. When the clear flange was bolted on to the chamber, rubber seals were used for vacuum sealing. The Bayonet Neill–Concelman (BNC) connector is fitted onto the clear flange and used to route cables to the module to amplify signals from the beamstop so that it can be recorded from the data room.

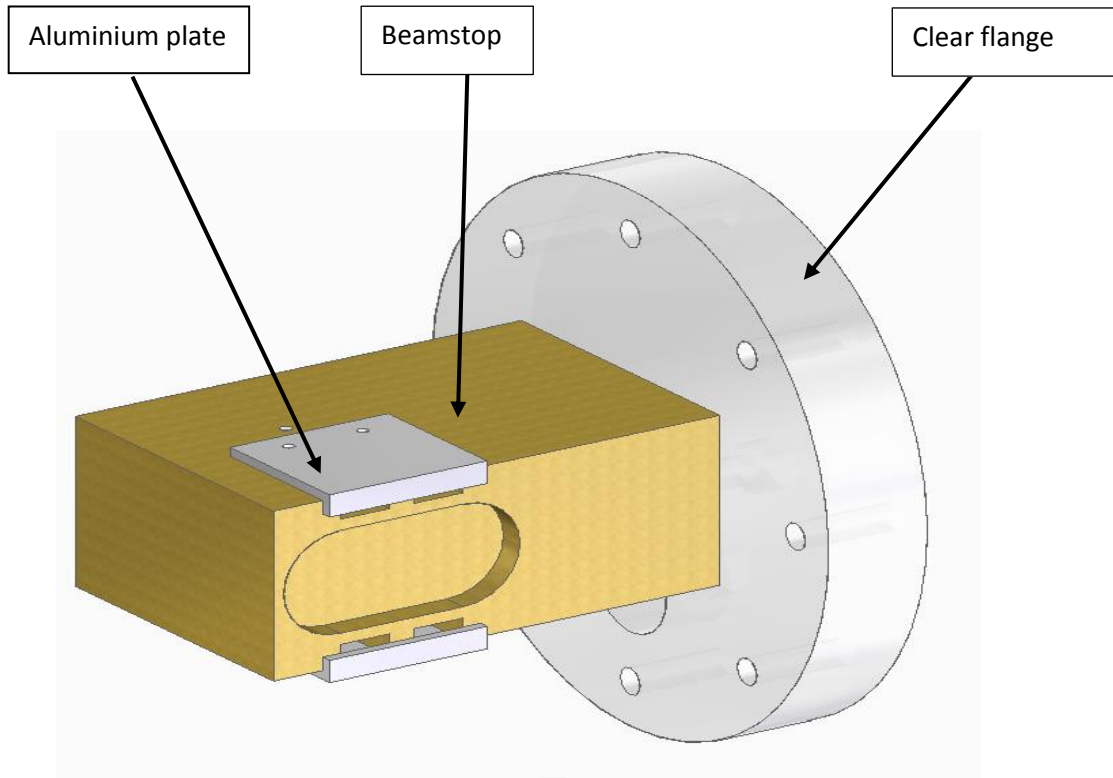


Figure 2.2: Beamstop with clear flange.

There are several beamstop configurations which can be used at the K600 magnetic spectrometer namely; external beamstop for $\theta_{K600} > 21^\circ$, internal beamstop for $5^\circ < \theta_{K600} < 21^\circ$, internal beamstop for angles $2^\circ < \theta_{K600} < 5^\circ$, $\theta_{K600} = 0^\circ$ beamstop for (p, p'), and $K600 = 0^\circ$ beamstop for (p, t). With p being a proton, p' a scattered proton, and t a triton. (P, p') is a reaction whereby a beam of proton scatters elastically from target and (p, t) is when proton knock off a neutron from the target and become a nucleus with proton and neutron. The choice of the K600 magnetic spectrometer angle and where the beamstop should be positioned is related to the type of the scattering chamber. Over the years there has been different scattering chambers used at the K600. Figure 2.3 shows the first scattering chamber used in the K600 magnetic spectrometer when it was commissioned for the first time in middle of the 1990's.

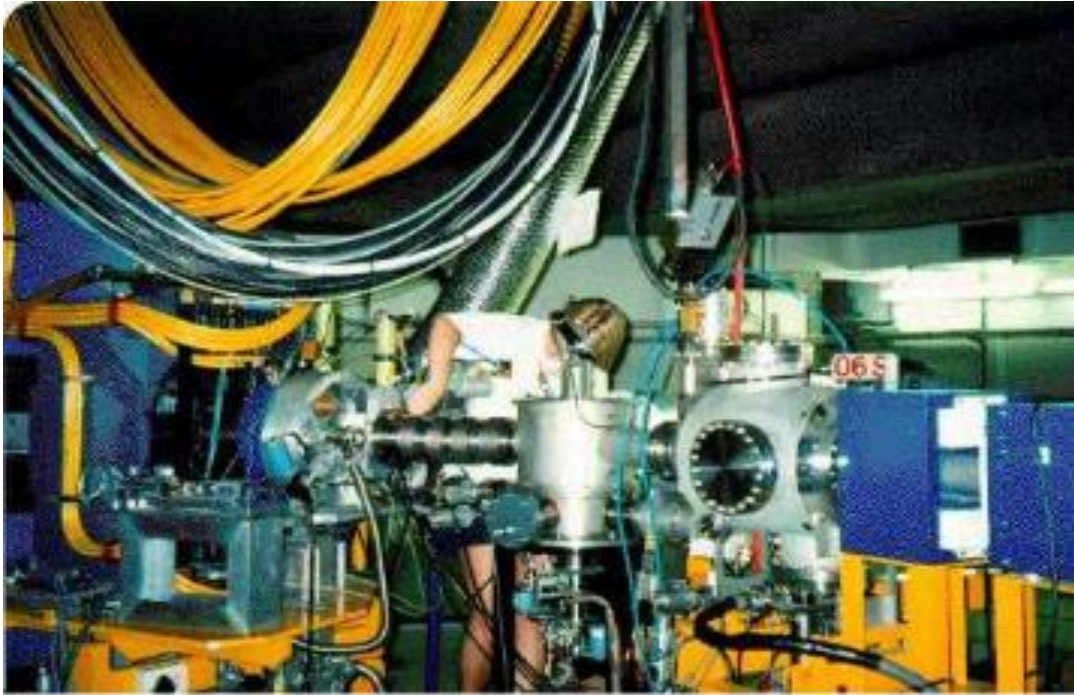


Figure 2.3: First scattering chamber in the middle 1990's.

From a research done by Cowley and Neveling at iThemba LABS there was a slight improvement from the first scattering chamber. See figure 2.4 for the improved scattering chamber used from 1999.



Figure 2.4: The scattering chamber used from 1999.

By the year 2014 and 2015 two scattering chambers shown in figure 2.5 and 2.6 were commissioned and are currently being used at the K600 magnetic spectrometer. When running an experiment the operator gets to select either the coincidence array for K600 experiments (cake) or sliding seal scattering chamber depending on the experimental requirement. The cake is a silicon array for use with the K600. The sliding seal scattering chamber is used when running experiments of angles greater than 6° while the cake scattering chamber is used for small angle experiments between 0° to 6° . The cake scattering is the preferred choice as it is made out of thin aluminum which allows detectors to read results easily compared to the stainless steel of the sliding seal scattering chamber. The entire K600 magnetic spectrometer can be rotated around 360° and it's one of the few high energy spectrometers in the world.

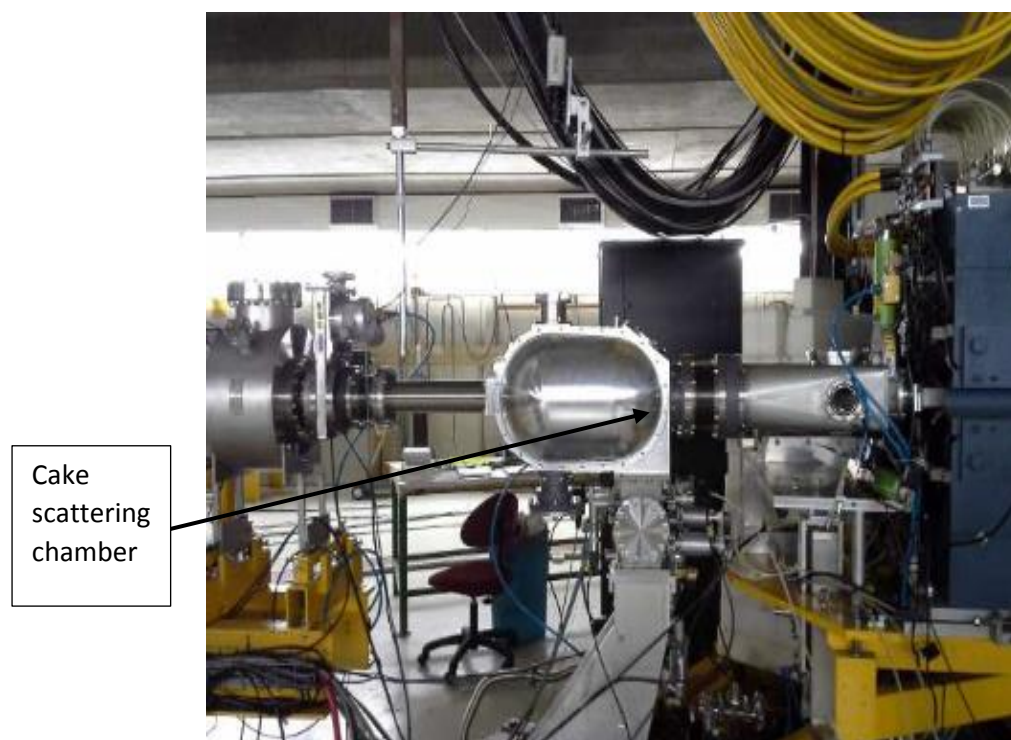


Figure 2.5: The cake scattering chamber during its commissioning run in 2014.



Figure 2.6: The sliding seal scattering chamber in 2015.

2.3 Collimator holder

The collimator holder was designed to accommodate three different collimators as shown in figure 2.7, with a solid collimator in the middle and not interchangeable. Only the top and bottom collimators will be used for inserting different collimator-inserts. The holder is made out of vesconite because of the need to electrically isolate the outside chamber from the collimators to prevent interferences with data collection. The side dove-tail guide is used for the sliding of the ladder up and down during positional drive. On the opposite side where the beamstop is located a mark was required to give operator a physical point to double check when the collimator is close to alignment with centre of the beam during experiment preparations.

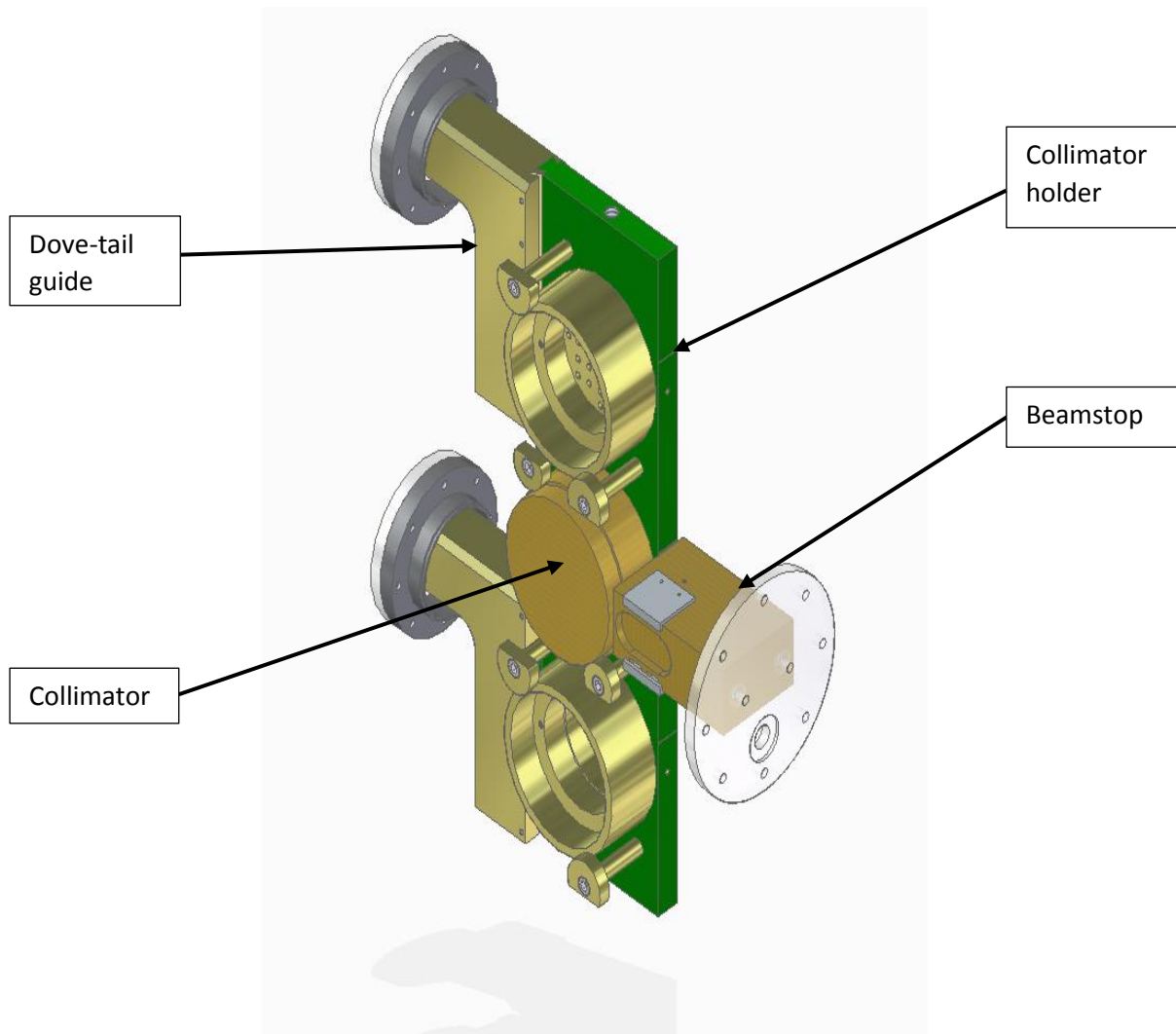


Figure 2.7: Collimator holder.

2.4 Model design

When designing the prototype the client/end user requirements were taken into consideration. Before manufacturing process, simulation was done to test and validate the design. Details of the simulation are discussed in chapter three. All manufacturing/ technical drawings were done according to international organisation for standardisation (ISO standard). See appendix B for detailed drawings and the full assembly.

2.5 Positioning system

Force and power of fluids like water, oil and air are commonly used in positioning systems or automation systems (Magdziak et al., 2016). Systems that use air are called pneumatic systems while those that uses liquids are called hydraulic systems. In this study a pneumatic system is utilised. The pneumatic system makes use of compressed atmospheric air and this

air is clean which means that it does not cause contamination to the system as compared to the hydraulic system. Compressed air is the normal air that gets squeezed in a small space under pressure, and this under pressure air retains potential energy which can be released to do work. Pneumatic drives are widely used in robotics and automation systems because they are easy to maintain, clean, and reliable with cost effective components.

The software used to remotely control linear positioning (Pneumatics) interfaces with experimental physics and industrial control system (EPICS). Reason for using EPICS was because it's a free open source software. iThemba LABS is paying lot of money for licencing soft-wares like Laboratory Virtual Instrument Engineering Workbench (LabVIEW), hence they are moving the facility to EPICS to cut costs.

In 1988 Epics was started at Los Alamos National Laboratory (LANL) during the accelerator automation application tool-kit workshop. In August 1993 the first epics website came online and according to Dalesio L.R (1989: 288-291) Epics can do any typical distributed control system function, for example:

- Remote control and monitoring of technical equipment
- Data conversions and filtering
- Closed loop control, both slow and fast
- Access security
- Equipment operation constrains
- Alarm detection, reporting and logging
- Data trending, archiving, retrieval and plotting
- Automation sequencing of operations
- Mode and facility configuration control
- Modelling and simulation
- Data acquisition and analysis.

2.5.1 Pneumatic air motor

A pneumatic air motor drive is utilised for this study and this type of motor works on the basic principle of expanding compressed air to do mechanical work, which is linear motion in this study. The motor was selected because the prototype operates under radioactive environment, and it has minimal electronics, which makes it suitable for this application and environment. Refer to the motor specifications listed in table 2.1 for model and operation power.

Table 2.1: Motor specifications.

Motor code	187213202
Model	MO20R
power	645 Watts
Speed at the max power	100rpm
Torque at the max power	77Nm
Static torque	90Nm
Idle speed	200 rpm
Air consumption at max power	18 l/s
Weight	4.8 kg

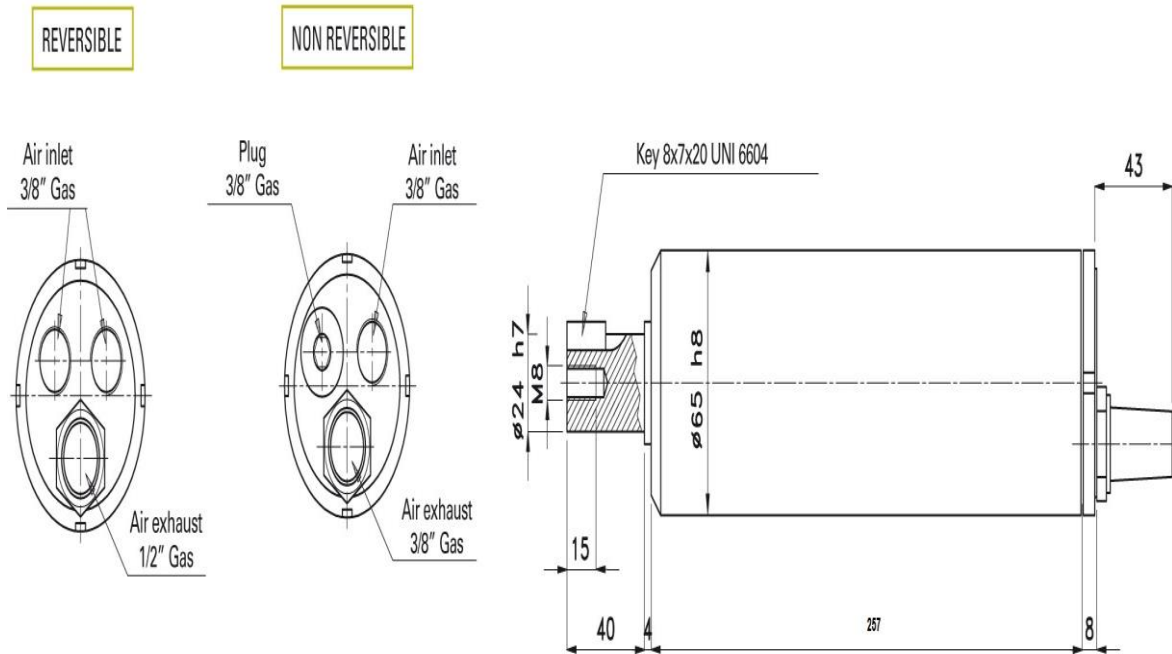


Figure 2.8: Motor dimensions (Langro, 2011).

Figure 2.8 gives the motor dimensions which were essential for process of purchasing pneumatic fittings.

2.5.2 Valves

2.5.2.1 Solenoid valve

The system makes use of a 5/3 – way solenoid valve as shown in figure 2.9. The mid-section of the valve is closed, allowing no air flow into the system. The valve can be actuated on either side, activating either inlet one or inlet two. The two inlets run at different directions, one is responsible for clockwise and the other counter clockwise rotation of the rod screw. The specifications of the valve are summarised in table 2.1.

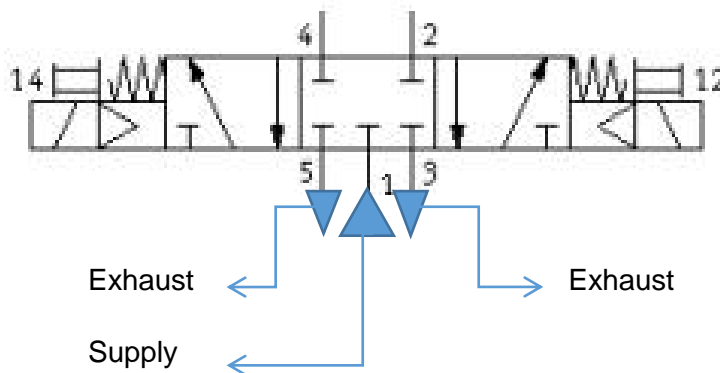


Figure 2.9: Schematic of the 5/3 – way valve (Festo, 2018).

Table 2.2: Valve Specifications.

Operating Pressure (bar):	3 to 8
Operating temp. (°C):	-5 to +50 (+60 with holding current reduced)
Operating Voltage(VDC):	24 ± 10%
Air Quality:	ISO 8573-1:2010 [7:4:4]
Corrosion resistance classification CRC:	2

2.5.2.2 Flow control valve

The flow control valve shown in figure 2.10 was utilised to regulate the flow or air pressure from the solenoid 5/3 – way valve to the pneumatic motor. To aid the programming of the system, the flow control valves used are solenoid speed valves as they are electromechanically operated. To assist the speed control valves with achieving accurate positioning, an electric pressure regulator is used to control the pressure of the air from the supply. These controls regulate the force that the air flows into the system.

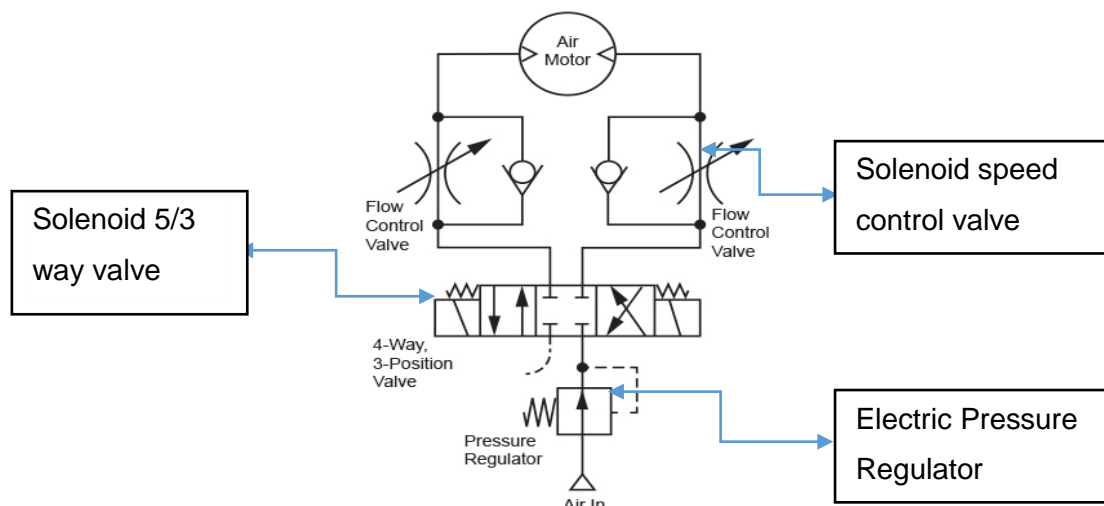


Figure 2.10: Automated pressure control with solenoid alternatives. (Womack, 1990).

2.5.3 Linear potentiometers

Linear potentiometer (POT) was used in this study for accurate positioning of the collimators onto the beamline. It is utilised due to the fact that it produces a resistance output that varies according to the displacement or position of a slider or wiper. Refer to figure 2.11 for the POT being utilised which is mounted on to the chamber and the sliding plate driving the ladder rod. With every movement of the sliding plate, the voltage of the potentiometer is altered respectively.



Figure 2.11: Linear potentiometer (Festo, 2018).

Limit switches will be used to restrict the distance travelled by the POT so that it stop at the outermost point (for the alignment of all three collimators to the beamline).



Figure 2.12: EL2808 – Linear Solenoid Switch (Rs components, 2018).

CHAPTER 3

Modelling and Simulation Study

3.1 Introduction

Simulation was developed during the time of World War II by two mathematicians Jon Von Neumann and Stanislaw Ulam, but it was only in 1984 that the first simulation language designed specifically for modeling manufacturing systems was developed (Fontana, 2005).

The aim of simulating the design was to verify and validate the intended function of the model; hence various simulations were carried out for the complexity of the application environment and the required accuracy. Simulation is a set of mathematical equations signifying the performance of the system in a physical field of interest and its complexity depend on data availability and varies in function of the application.

3.2 Design simulation software

The Solid Edge CAD software is utilised for this study to simulate the model and the results obtained are discussed in chapter four. Solid Edge was used instead of other simulation software like Abaqus because of its availability at iThemba LABS.

3.2.1 Finite element analysis.

Finite element analysis (FEA) is a method that helps to simulate mechanical parts and systems to get information about failure, deformation and stresses under different types of loading. It can help mechanical designers to create more robust and enhanced products. FEA is also useful to easily detect causes of failure in a system and make the system safer by evaluating the risks of failure under various loading conditions.

FEA can solve large complex problems by breaking the structure down into smaller simpler pieces. It uses matrix algebra to solve simultaneous equations by connecting elements to each other by nodes, and for each different node a number of questions exist. Set of equations which can be used for hand calculations are as follows (Naude, 2017).

$$F_x = K_x \cdot U_x \quad (1)$$

Where F_x is the applied force vector (N), K_x is the global stiffness matrix (N/mm), and U_x is the nodal displacement vector (mm).

$$\varepsilon = \frac{\Delta L}{L} = \frac{u_2 - u_1}{L} \quad (2)$$

Where ε is Strain, and $\frac{\Delta L}{L}$ is the displacement

Figure 3.1 shows a typical FEM process on Solid Edge:

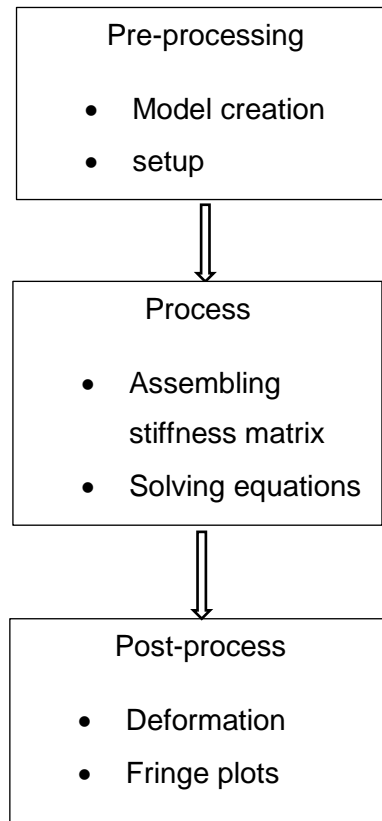


Figure 3.1: FEM process in Solid Edge.

When considering the use of FEA the right questions needed to be answered first like; what a designer want to know or the results designers are interested in as well as the accuracy of the results required in critical components. And some of the answers which were acquired from those question where; the type of analysis to conduct and the important results to save or accept for the design.

3.2.2 Analysis procedure

For this study a linear static analysis is carried out and briefly described with preliminary calculation formulas and software simulation later on. Linear statics is used to get results of forces, moments, stress, strain and deflection. With linear statics the load does not move out of location but stays inline whereas with non-linear static a point to apply load is chosen. It is most accurate if the deflection is small and varies slowly.

3.2.2.1 Buckling analysis

Buckling may lead to failure mode when a structure is subjected to compressive stress. Buckling is characterised by a sudden sideways deflection of a structural member. It works on the basis of having applied a load on top and the gravitational load interacting at the bottom. It uses the mode shape of the structure to predict the buckling shapes, and the load factor multiplied by the applied load gives the critical buckling load (i.e. Buckling load= applied load x load factor). If the load factor is ≥ 1 it means the buckling point has been excited, meaning that chances of it buckling or failing are low. Linear buckling is similar to theoretical Euler buckling (Drotsky, 2011):

$$P = \frac{\pi^2 EI}{(KL)^2} \quad (3)$$

P= Euler critical load, E = modulus of elasticity of material, I= minimum area moment of inertia, K= effective length factor, L= length.

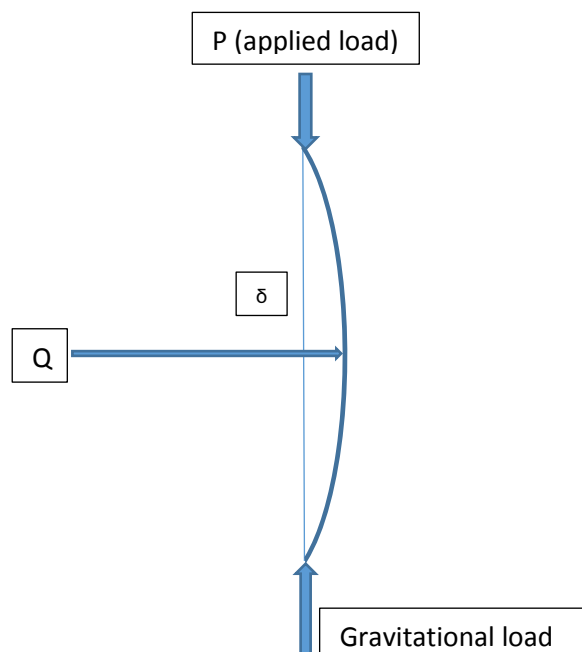


Figure 3.2: Buckling beam.

Q being the lateral force which results in displacement (δ) shown in figure 3.2. If the displacement disappears when the lateral force is removed, then the critical load has not been reached because the critical load is defined as the load at which the lateral displacement does not change after removing the lateral load (Drotsky, 2011).

3.2.2.2 Linear stress analysis

When designing with the CAD software linear stress analysis enables the designer to easily and efficiently validate the quality, performance of the model, and safety while still creating the design before manufacture. In the design process, one can determine when the design will fail if the maximum value of Von Mises stress induced in the material is more than the strength of the material. When the material is ductile the Von Mises works well and it can be calculated using the following formula (Budynas & Nisbett, 2009)

$$\sigma = \sqrt{\frac{1}{2}(\sigma_1 - \sigma_2)^2 + (\sigma_2 - \sigma_3)^2 + (\sigma_3 - \sigma_1)^2} \quad (4)$$

Where $\sigma_1, \sigma_2,$ and σ_3 of equation 4 are the principal stresses. Using figure 3.3, one can analyse how the material behaves, be able to determine whether is brittle or is ductile, and also be able to determine the loads that it can withstand before it fails. The curve is basically used to predict the behaviour of the material.

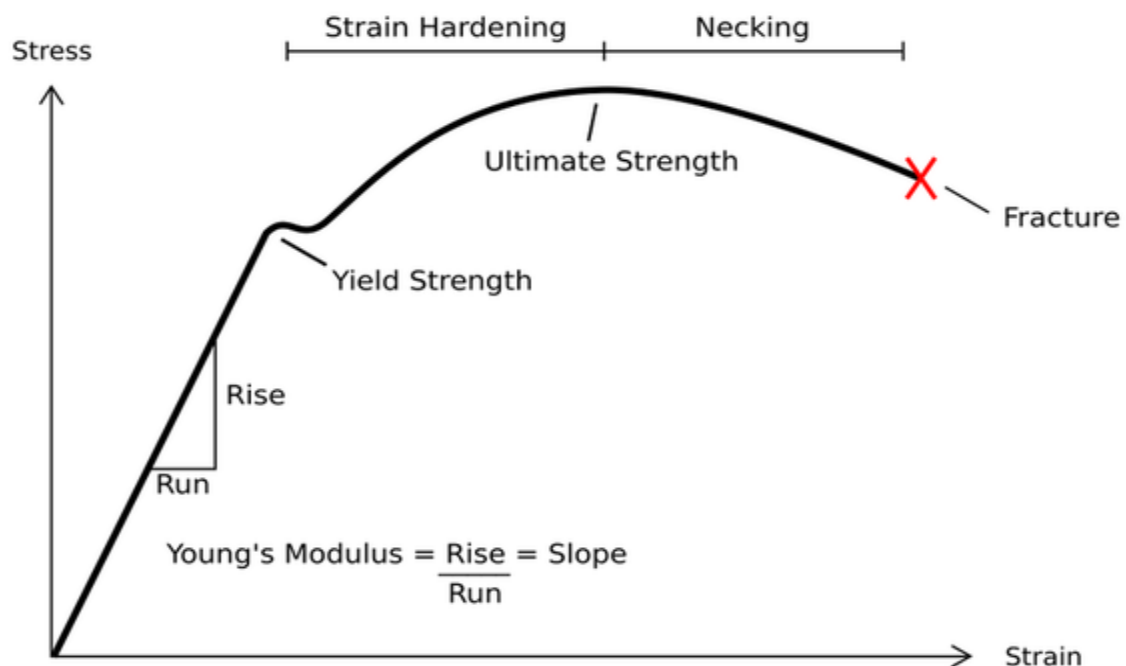


Figure 3.3: Stress strain curve to analyse material properties (Philipfigari, 2015).

CHAPTER 4

Simulation results and discussion

4.1 Simulation results

In this chapter results from Solid Edge simulation are presented and discussed in detail. The results presented here are for crucial components on the model design and the model needed to withstand applied load and also meet the required vacuum of 10^{-8} mbar. When running the simulation the following data was applied: Atmospheric pressure of 101Kpa was utilised for simulation chamber for vacuum reasons. An axial load of 68.38N obtained from equations 5, was used for simulating pillars to observe stress, strain and buckling. The load applied was calculated from the weight of the motor combined with the holding plate weight. Motor weight was obtained from the specifications in figure 2.1 to be 4.8 Kg, and the weight of the plate was obtained from Solid Edge software to be 2.17 Kg which is related to the material density and thickness.

$$F = m \times a \tag{5}$$

$$= (4.8 + 2.17) \times 9.81$$

$$= 68.38 \text{ N}$$

4.1.1 Chamber Body results

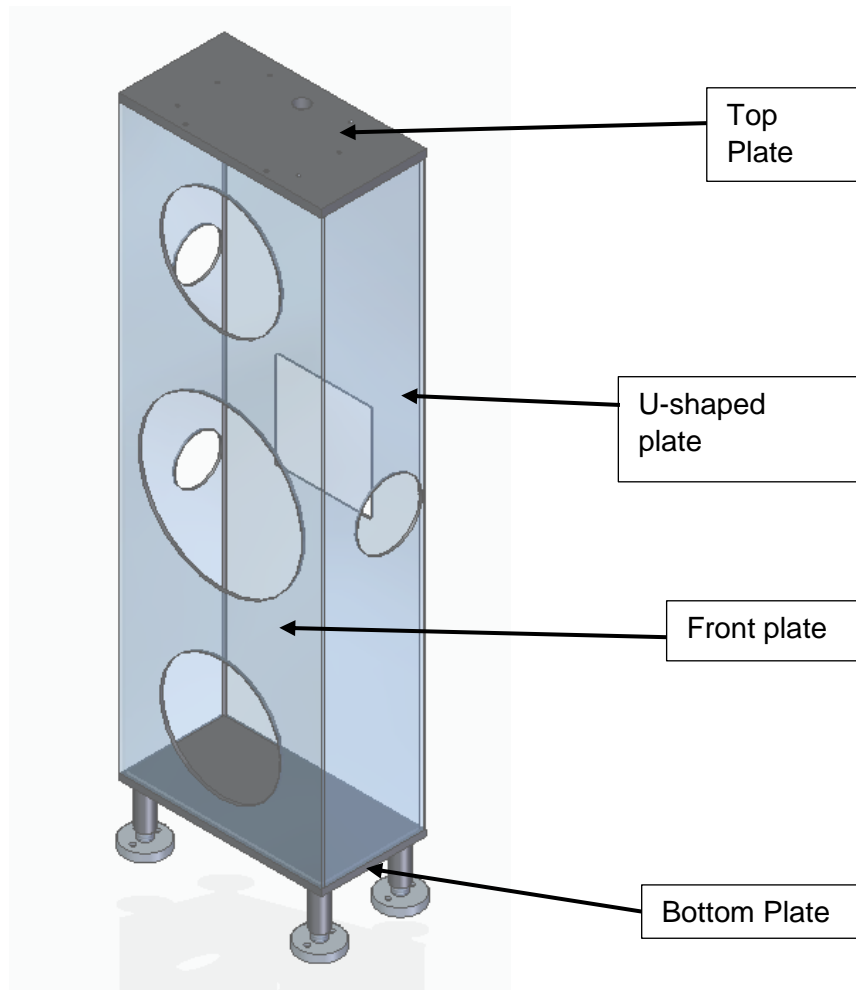


Figure 4.1: Chamber body.

For the chamber body, stainless steel 316L was used because of its non-magnetic property. The stainless steel was considered suitable for the chamber body since the body required welding and the stainless steel 316L non-magnetic effect makes it easy to weld and also helps with reducing distortion as it does not require being heated for long when welding. The chamber simulation was essential and needed to be performed because the chamber operates under vacuum, thus it was simulated to observe how it would react under a vacuum of 1×10^{-8} mbar. The chamber body was made out of four parts as seen from figure 4.1 namely, the u-shaped plate which is 3mm thick, the flat front plate which is 4mm thick, and the top and bottom plate which were 10mm. all four plates were joint by welding to form a chamber. The front plate was made 1mm thicker than the u-shape since it required more welding where the three holes opening are. Table 4.1 gives characteristics of the four parts of chamber body.

Table 4.1: Characteristics of Chamber's parts.

Part	Material	Mass (Kg)	Volume (mm³)	Weight (N)
U-shaped plate	Stainless steel 316L	7.99	996208.63	78.37
Front plate	Stainless steel 316L	3.60	448527.91	35.28
Top plate	Stainless steel 316L	2.54	315915.96	24.85
Bottom plate	Stainless steel 316L	3.04	378764.45	29.80

The atmospheric pressure of 101Kpa was applied as external load, and on the internal a vacuum of 1×10^{-8} mbar was applied to the body during the chamber simulation. The chamber was constrained using bolts on its four legs in order for the simulation to be fully defined on Solid Edge. The welding was represented by stitching the plates together. All this had to be done in order for the software mesh and solve the simulation as the design need to be fully defined in order to see where failure occurs.

Table 4.2: Properties of stainless steel 316L from Solid Edge data base.

Property	Value
Density	8027.000 kg/m ³
Thermal Conductivity	0.017 kW/m-C
Specific Heat	502.000 J/kg-C
Modulus of Elasticity	193053.196 MPa
Poisson's Ratio	0.290
Yield Stress	248.211 MPa
Ultimate Stress	530.896 MPa

Density of a material is important to the simulation study process because it measures how heavy an object is and the weight of the object can affect the overall design if not taken into consideration when designing, by either over designing which can lead to failure. Thermal conductivity is an essential property because it measures the rate at which heat is transferred through a material. The environment where the prototype operates in will not be affected by any temperature rise, as all hot equipment are always cooled down using liquid nitrogen during experiment.

The specific heat of material is critical when designing systems where the management of heat is essential to avoid overheating of the system. Modulus of elasticity is important for the design in order to know the stress the material can undergo without getting permanently deformed. Poisson's ratio represents an event where the material is compressed in one direction but tends to expand in the opposite direction perpendicular to the direction of compression. If the Poisson's ratio for the material is not defined, simulation will assume that Poisson's ratio is equal to zero which provides inaccurate results.

When designing components the yield stress is important because components need to carry a certain load without undergoing a plastic deformation. Yield stress is the point where the material begins to plastically deform (Drotsky, 2011). The ultimate stress is the maximum stress that the material can withstand while being pulled or stretched before actual failure of the material.

4.1.1.1 Linear static analysis

In linear static analysis two assumptions are made. First the relationship between the applied load and the reaction of the structure is linear, second this relationship does not depend on time. When simulating linear static analysis on Solid Edge the software solves linear equations.

The linear static analysis was used when simulating the chamber to obtain the displacement, factor of safety and stress results. Results obtained from these analysis helps to prevent failure because the software helps one to visualise where failure can occur first. If one finds the cause of failure before manufacturing, modifications can be done in cases where the material can be changed to use stronger material or change thickness to reduce displacement.

Table 4.3 gives the maximum displacement value of 2.88mm and the minimum of 0mm the chamber will experience. The x, y, z coordinates represents the original location of node where the maximum and minimum displacement is taking place.

Table 4.3: Chambers displacement results.

Extent	Value	X	Y	Z
Minimum	0 mm	-125 mm	-67 mm	360 mm
Maximum	2.88 mm	0 mm	61.50 mm	-60 mm

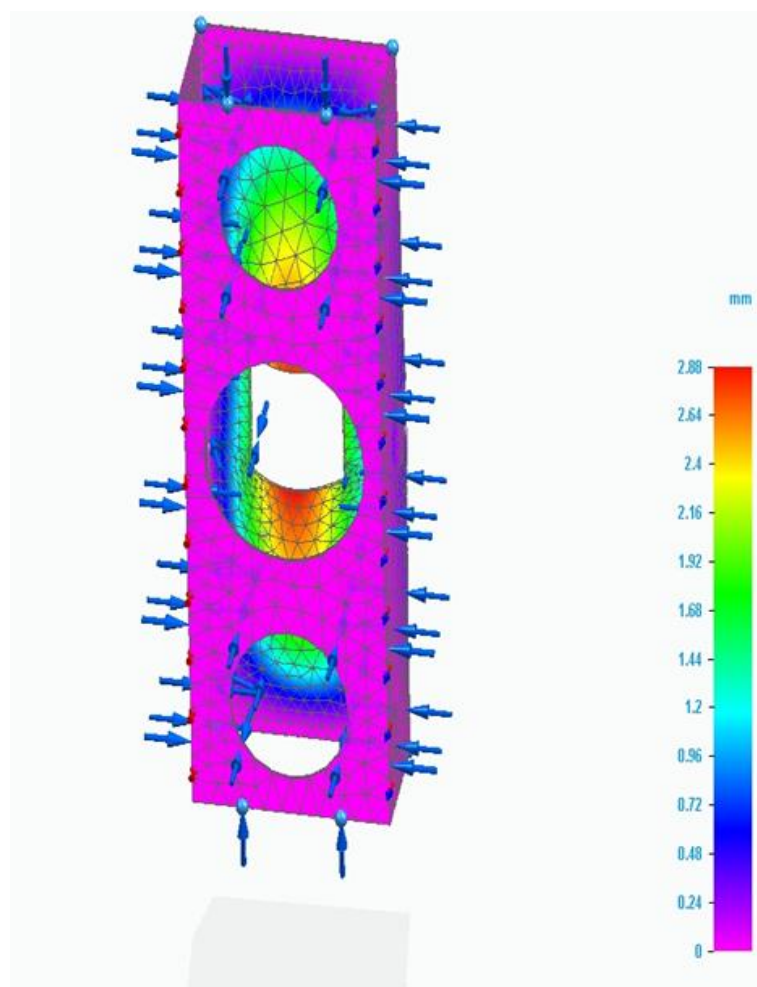


Figure 4.2: Chamber displacement.

Figure 4.2 shows the chamber displacement distribution. It was noticed that the maximum displacement the chamber can experience under applied atmospheric pressure of 101Kpa is 2.88 mm. The chamber experiences this maximum displacement at the back plate shown in red colour on figure 4.2. The red part experiences this displacement because of the square cut-out. This is due to the fact that square corners are weak compared to round corners.

Table 4.4 gives the maximum and minimum stress values that the chamber experiences under applied pressure. As mentioned earlier the x, y, z coordinates represents the original location of node where the minimum or maximum stress is experienced.

Table 4.4: Chambers stress results.

Extent	Value	X	Y	Z
Minimum	0.499 MPa	0 mm	-63 mm	101.75 mm
Maximum	198 MPa	125 mm	43.85 mm	31.41 mm

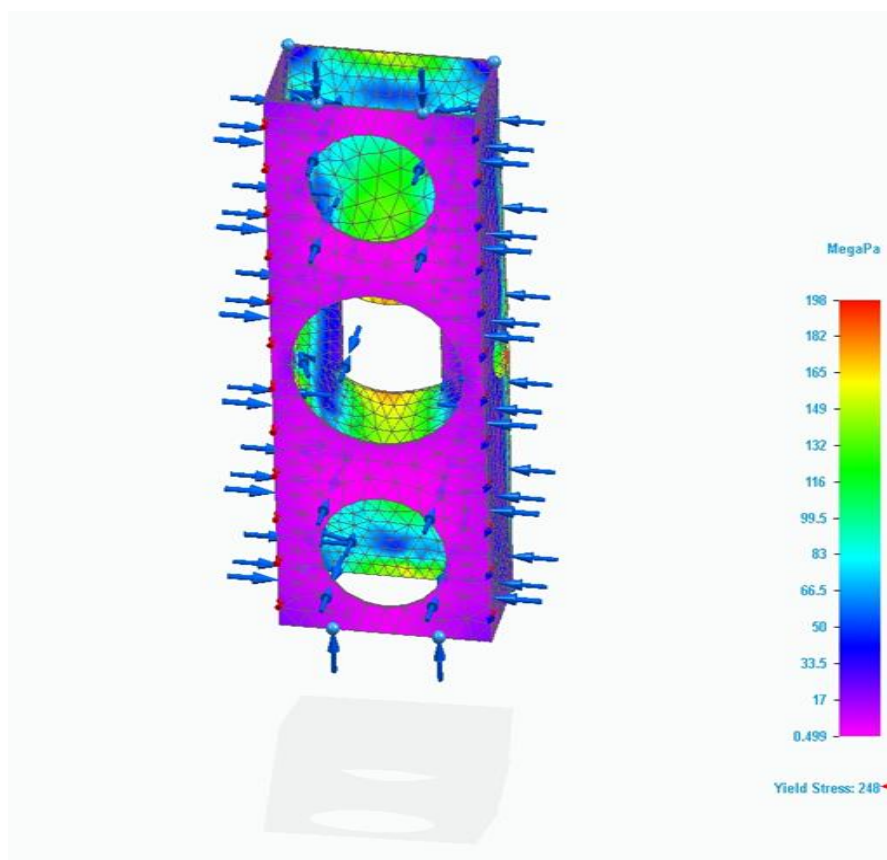


Figure 4.3: Stress results.

The stress results in figure 4.3 were observed and it was noticed that the maximum stress the chamber will experience under pressure is 198MPa. The areas that experience this higher stress can be noticed in red colour at the back and this is because of the square cut-out because the corners experiences more stress. With the maximum stress less than the ultimate stress of 530.39MPa given in table 4.2, it is safe to say the chamber will not break and also with the yield stress of 248MPa less than the maximum stress experienced by the chamber it was concluded that the chamber is safe from deforming permanently.

The factor of safety is the ratio between the strength of the material and the maximum stress experienced by the structure.

$$\text{Safety factor} = \frac{\text{strength}}{\text{maximum stress}} \quad (\text{Drotsky, 2011}). \quad (6)$$

The factor of safety less than one represent likely failure, whereas greater than one represents how much the stress is within allowable limit.

Table 4.5: Chambers factor of safety results.

Extent	Value	X	Y	Z
Minimum	1.25	125 mm	43.85 mm	31.41 mm
Maximum	497	0 mm	-63 mm	101.75 mm

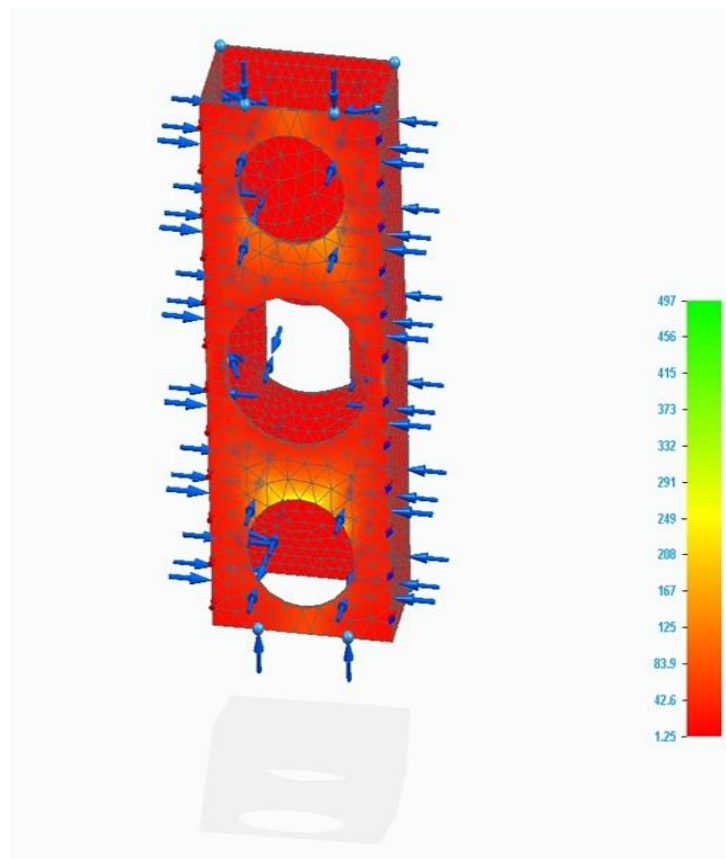


Figure 4.4: Factor of safety results.

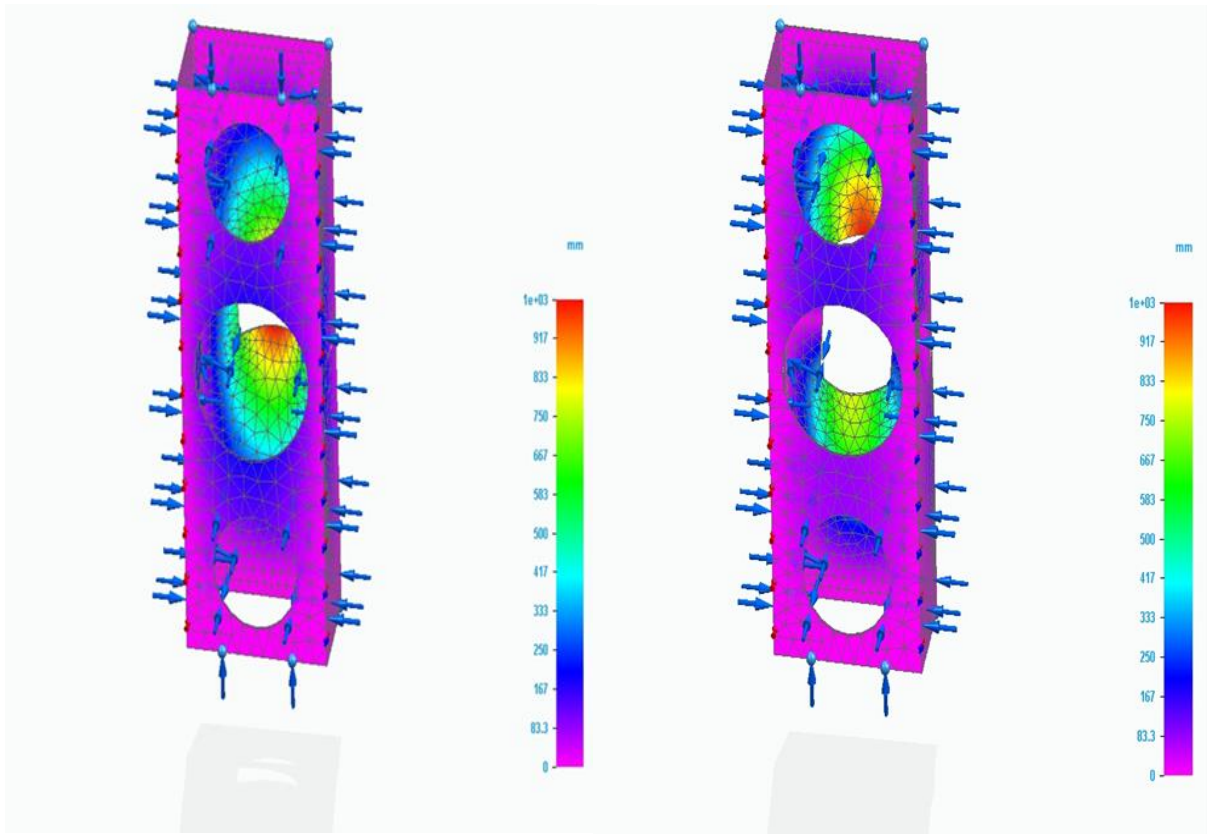
From figure 4.4 it was noticed that the FOS is greater than one and from that observation, the chamber was regarded safe as it is far from likely failing under pressure. The minimum value in table 4.5 is greater than one which justify how safe the chamber is under atmospheric pressure.

4.1.1.2 Eigenvalues buckling analysis

The load magnitude which causes buckling was calculated using eigenvalues buckling on Solid Edge simulation. Eigenvalue buckling only provide the shape the structure assumes when it buckles in a particular mode hence it only gives strain results and not stress. Table 4.6 presents four mode results that the structure assumed for buckling under applied pressure. A mode is a combination of a deformed shape in which the structure will exchange kinetic-energy and strain-energy continuously, and the natural frequency at which the mode shape occurs (Naude, 2017).

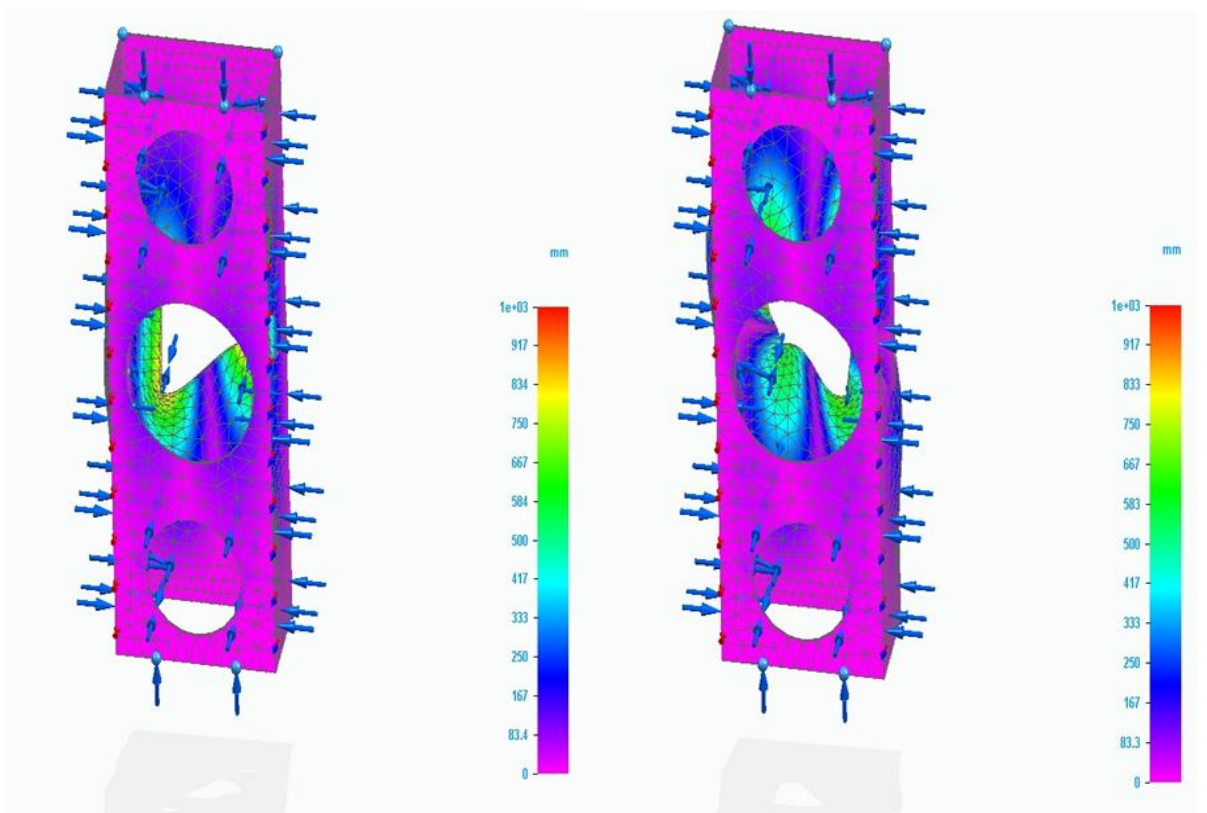
Table 4.6: Buckling results.

Result component: Total Translation in (mm)				
Extent	Value	X	Y	Z
Mode 1, Eigenvalue: 14.72				
Minimum	0	-125	-67	360
Maximum	1X10 ³	0	61.5	-60
Mode 2, Eigenvalue: 18.47				
Minimum	0	-125	-67	360
Maximum	1X10 ³	0	61.5	60
Mode 3, Eigenvalue: 26.87				
Minimum	0	-125	-67	360
Maximum	1X10 ³	60	63	-21.38
Mode 4, Eigenvalue: 30.75				
Minimum	0	-125	-67	360
Maximum	1X10 ³	49.88	61.5	60



Mode 1

Mode 2



Mode 3

Mode 4

Figure 4.5: Eigenvalue buckling results.

As mentioned before the eigenvalue buckling study provide only the shape the chamber assumes when buckling. From figure 4.5 four different modes were observed to visualise the shape the chamber is likely to assume when under strain. From these modes it was noticed that the eigenvalue increases with each mode. Only a few modes are presented from the Solid Edge software because it gives same value for the strain, the only difference we get is the shape as the software try to show all possible shapes the chamber can take.

From both the mode the chamber shape presents the strain at similar point which is the cut-out plate with corners for the reason mentioned previously of weak area around corners. It can be concluded from the shape and the strain value that the only weak area is the corners and this area will not deform plastically under pressure as the deformation and stress the chamber experiences is within the factor of safety allowable limits.

4.1.2 Motor drive results

The motor drive was simulated to observe the behaviour of pillars under axial load, i.e. the motor weight (4.8kg) combined with the stainless steel plate and the motor clamp on top of the pillars shown in the figure 4.6.

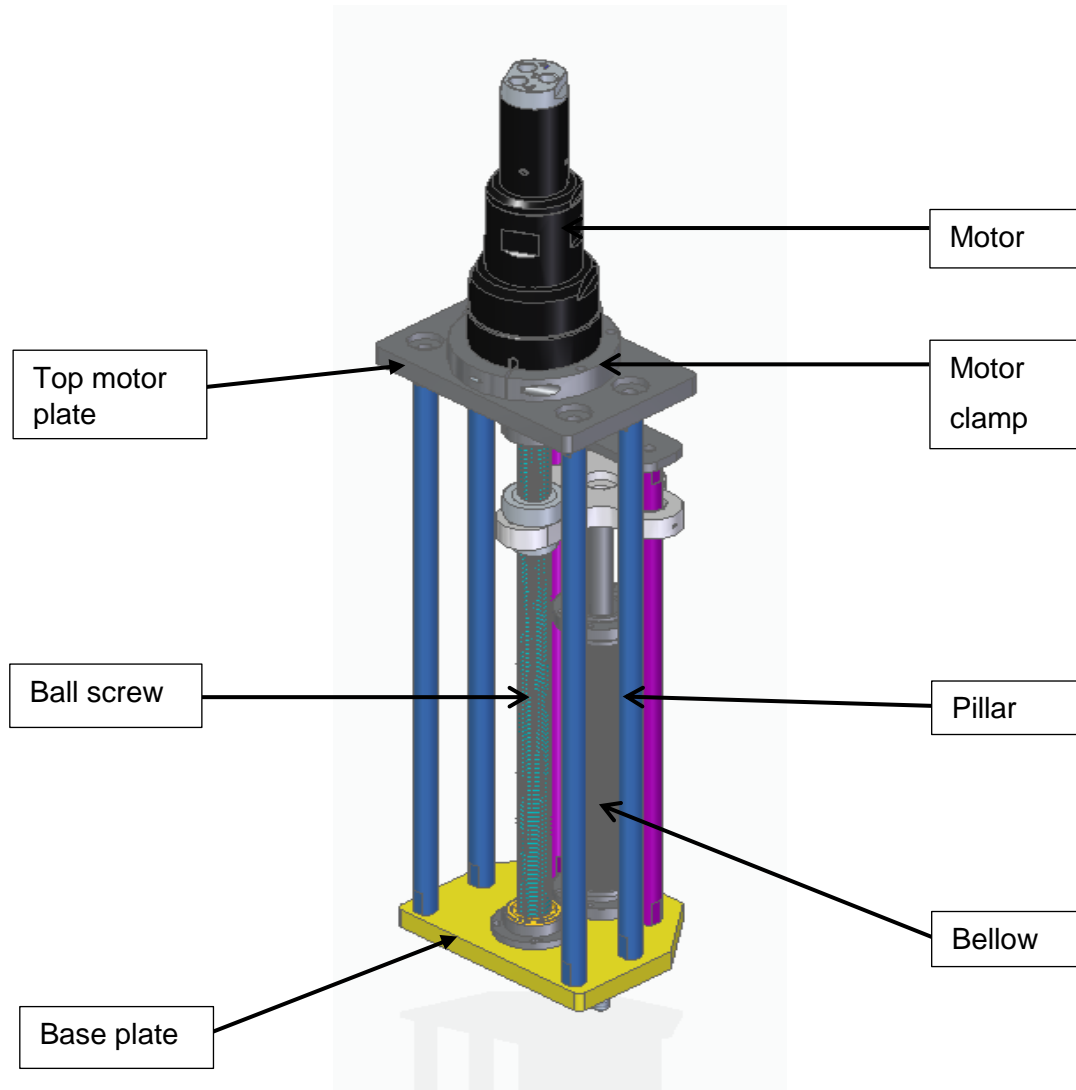


Figure 4.6: Drive assembly.

For the motor drive assembly, different materials were utilised depending on the application of the part. For the motor clamp, Aluminium was used, and the main reason to use aluminium was to avoid rubbing on the motor and damaging it. Stainless steel 316 and stainless steel 304 were used for other parts of the assembly. The base plate shown in colour yellow in figure 4.6 gets bolted on top of the chamber and it has O-ring groove for vacuum sealing.

Table 4.7 gives details of all parts and their material property. The properties of stainless steel 316 were given previously in table 4.2 and those for Aluminium 1060 and stainless steel 304 are given in table 4.8.

Table 4.7: Characteristics of drive assembly parts.

Parts	Material	Mass	Volume	Weight
Guide rod	Stainless Steel, 304	0.630 kg	78513.899 mm ³	6.176 N
Drive plate	Aluminium, 1060	0.329 kg	121156.628 mm ³	3.220 N
Pillar	Stainless Steel, 304	0.695 kg	86598.789 mm ³	6.812 N
Motor plate	Stainless Steel, 316	2.171 kg	270461.083 mm ³	21.276 N
Guide rod	Stainless Steel, 304	0.582 kg	72461.623 mm ³	5.700 N
Plate	Stainless Steel, 316	0.268 kg	33365.354 mm ³	2.625 N
Base plate	Stainless Steel, 316	2.326 kg	289783.000 mm ³	22.796 N
Pillar	Stainless Steel, 304	0.695 kg	86598.789 mm ³	6.812 N
Pillar	Stainless Steel, 304	0.695 kg	86598.789 mm ³	6.812 N
Pillar	Stainless Steel, 304	0.695 kg	86598.789 mm ³	6.812 N
Guide pillar	Stainless Steel, 304	0.582 kg	72461.623 mm ³	5.700 N

Table 4.8: Properties of Aluminium and Stainless Steel from Solid Edge database.

Property	Aluminium 1060	Stainless Steel 304
Density	2712.000 kg/m ³	8027.000 kg/m ³
Thermal Conductivity	0.221 kW/m-C	0.017 kW/m-C
Specific Heat	920.000 J/kg-C	502.000 J/kg-C
Modulus of Elasticity	68947.570 MPa	193053.196 MPa
Poisson's Ratio	0.330	0.290
Yield Stress	27.579 MPa	255.106 MPa
Ultimate Stress	68.948 MPa	579.160 MPa

With the material selected for different parts of the assembly, it was possible to observe the behaviour of the pillars under axial load using Solid Edge simulation. For the motor drive assembly only linear static analysis were carried out to obtain the displacement, stress and factor of safety results.

Table 4.9 gives the maximum and minimum displacement results the motor drive will experience under axial load of 68.38N obtained from equation 5. The x, y, z coordinates represents the original location of node.

Table 4.9: Displacement results of motor drive assembly from Solid Edge.

Extent	Value	X	Y	Z
Minimum	0 mm	-53.43 mm	-55.67mm	378.17 mm
Maximum	0.00124 mm	-5 mm	-54.5 mm	-92 mm

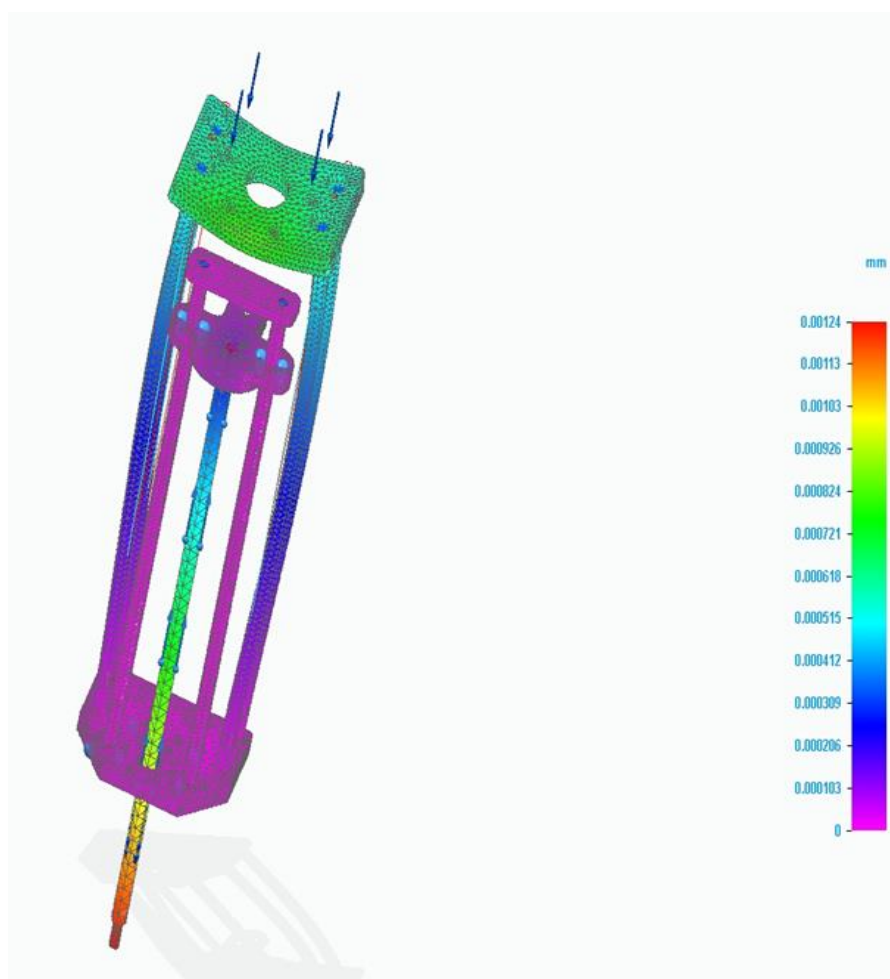


Figure 4.7: Displacement results of the motor drive.

The displacement results were observed from figure 4.7 and it was noticed that the point where the drive experiences maximum displacement is shown in red. The rod experiencing this maximum displacement is attached to the collimator ladder which accommodates three brass collimators. The weight of the ladder attached to the rod was assumed to be 10N by adding weight of the three collimators plus that of the ladder.

Table 4.10 gives the minimum and maximum stress in MPa that the drive experiences. The x, y, z coordinates represent the original location of node where the minimum or maximum stress is experienced.

Table 4.10: Stress results of the drive from Solid Edge.

Extent	Value	X	Y	Z
Minimum	1.61x10 ⁻⁹ MPa	-42 mm	-62 mm	428 mm
Maximum	0.99 MPa	5.25 mm	-54.5 mm	378 mm

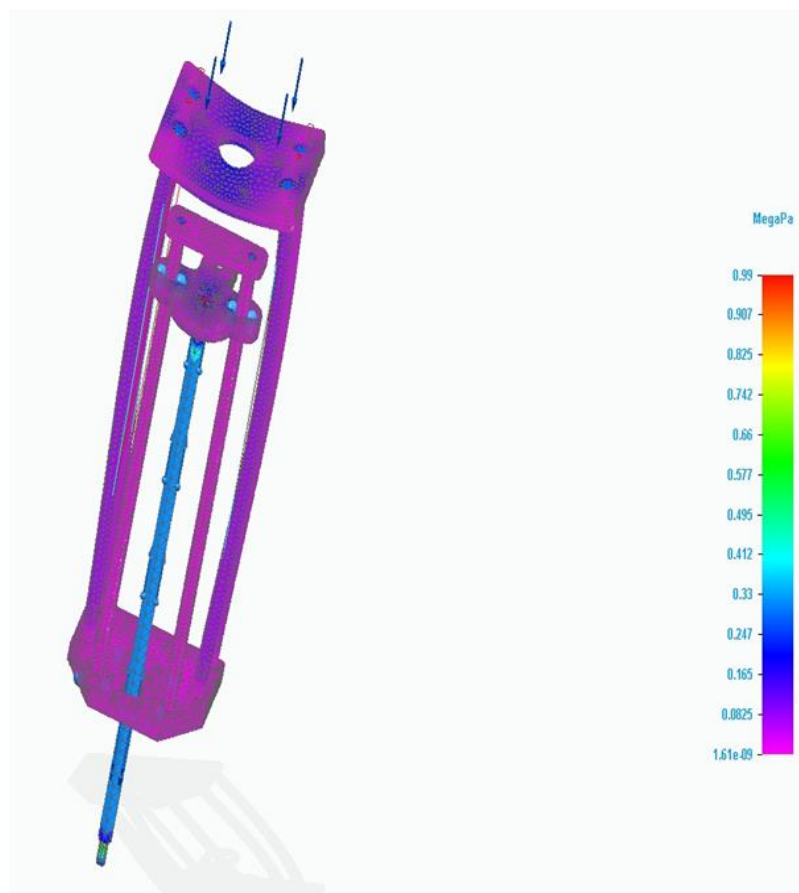


Figure 4.8: Stress results of the drive.

From figure 4.8 observations it was noticed from the contour bar that the maximum stress which can be experienced is 0.99MPa. The maximum stress it experiences is less than yield stress given in table 4.8 for both Aluminium and Stainless Steel. From this observation it was concluded that the drive is safe as it does not reach the ultimate stress of 68.95MPa for aluminium and 579.16MPa for Stainless Steel, where the material of the drive would break permanently.

Given in table 4.11 are the factor of safety parameters of the motor drive assembly, and location of the node on the model is represented by x, y, z coordinates obtained from Solid Edge.

Table 4.11: Factor of safety results from Solid Edge.

Extent	Value	X	Y	Z
Minimum	27.9	5.25 mm	-54.5 mm	378 mm
Maximum	1.59×10^{11}	-42 mm	-62 mm	428 mm

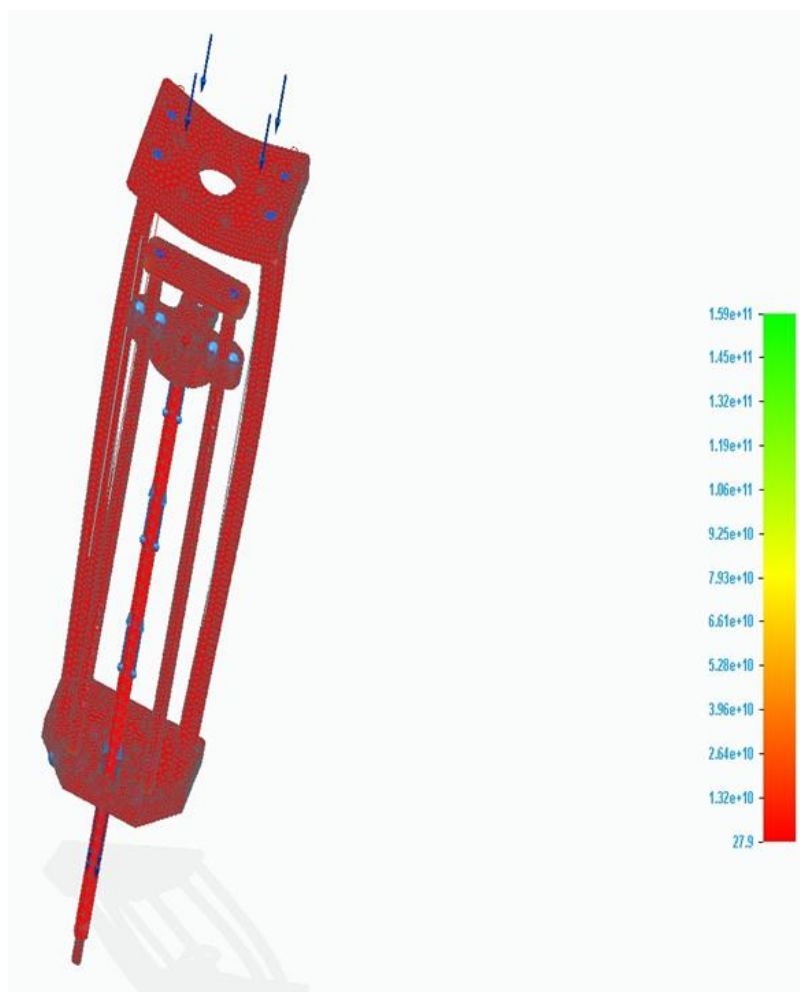


Figure 4.9: Factor of safety results.

The drive results shown in figure 4.9 were observed to see how safe the design is under applied axial loading. The red colour represents the minimum while green represents maximum factor of safety. With the drive red throughout it was regarded safe as the minimum factor of safety was greater than one.

4.2 Conclusion for this chapter

During the process of design simulation, it was noticed that the probabilities of components deforming under applied loads were minimal. Reason for this conclusion comes from the observation of the factor of safety, stress and displacement result. The results observations were important and had to be taken into consideration in order to avoid disaster where the component fails unpredictably.

This mechanism was designed with the assumed factor of safety of 2 to ensure that it is two times or more strong than the designed load. The factor of safety results obtained during simulation study for both chamber body and the motor drive were satisfactory. Similarly, the maximum displacement obtained from linear static and buckling analysis was considered minimal as the maximum stress experienced was less than the yield stress of the material. It was also noted that the eigenvalue load factor from table 4.6 was increasing with each mode. The four modes obtained from Solid Edge results helped to visualise the shapes the model is likely to take under strain. From the four modes presented it was noted that the chamber is weak at the square cut-out on the back plate hence the design uses more round cut-out than square ones for strength purposes.

CHAPTER 5

Assembly and installation of the model, Testing and validation

This chapter focuses on the assembly, installation, testing and the validation process of the prototype at the K600 magnetic spectrometer. Most of the components were manufactured on-site except for the products bought off-the-shelf, like ball screw and nut, pneumatic motor, electronics switches, etc. The process of manufacturing components on-site made it easy to machine and to also ensure that all the required tools for assembly were available and components that fit onto each other where manufactured to perfection by physically testing them together during the manufacturing stage. The assembly process was done in different stages before bringing everything together as one unit. This was done because of the height of the prototype being long to stretch; the chamber had lugs welded on its side for lifting purpose because the prototype is heavy and will require the use of lifting crane for installation onto the beamline. Figure 5.1 shows the overview of the prototype after installation. This chapter gives details of both assembly processes that took place for the top level unit as well as the chamber.



Figure 5.1: Prototype assembly.

5.1 Assembly of the motor drive mechanism:

The motor drive assembly (top unit) shown in figure 5.2 was done separately on the desk because it consisted of long pillars that needed to be bolted separate on the mounting plate before assembling it on top of the chamber for length reasons as it would have been difficult to mount the motor and its plate from high distance. The drive assembly holds the pneumatic motor with its shaft coupled to the ball screw that converts the rotational motion to linear motion through the ball screw nut. The linear motion from the nut drives the rod bolted to the ladder which holds three brass collimator to position (beam centre). Linear bearings were used to help drive the plate attached to the rod and the bearing were used to help the nut with the motion and alignment of the rod to the ladder to avoid friction and to achieve required accuracy.



Figure 5.2: Motor drive.

5.2 Chamber assembly



Figure 5.3: Chamber body.

Figure 5.3 shows the assembly of the chamber which accommodates the beamstop that is bolted on the stainless steel flange shown on the right hand side. The component where the beamstop flange bolts to is welded on the chamber body and it has an O-ring groove for sealing. The reason for bolting the beamstop on the side was to allow easy access when performing experiment which do not require the beamstop inside the chamber next to the collimator. The two dove-tail guides on the opposite side are bolted on the stainless steel flange in the same manner as the beamstop, whereas the valve adaptor plate located at the back is welded onto the chamber body. Assembling the chamber components was challenging as the guide and the collimator ladder needed to be alighted with the driving rod to avoid friction or misalignment when driving the ladder for positioning.

The O-rings were also crucial on the chamber assembly to ensure that the sealing is perfect around their grooves to avoid leaks. After assembly process was completed the prototype was installed at the K600 magnetic spectrometer vault. All the necessary components to operate prototype electronically were connected then the chamber had to be pumped down. The pumping down of the chamber was done to create vacuum of 10^{-8} mbar that the chamber needs to meet during experiment. When pumping down small leaks were found around bolted areas and they were fixed before the prototype was validated.

5.4 Control systems

Electronic controls were used for accurate positioning of collimators to the beamline. Figure 5.4 shows the algorithm of the electronics control. When remotely controlling the linear motor for positioning, the linear potentiometer is used for accuracy and the latches are used to lock position when the collimator is at the centre of the beamline. To avoid overshooting when driving the ladder up or down, two limit switches were installed. One installed at the maximum distance the ladder should travel and the other one at the minimum distance the ladder should not exceed.

Once the latches are actuated in the control system the position locked will stay constant unless changed. It is important to lock position when a desired location is reached to ensure the collimator does not move off the beam centre during experiments. A latch is an electronic logic circuit that has two stable states and can be used to store state information (Sedcole, 2008).

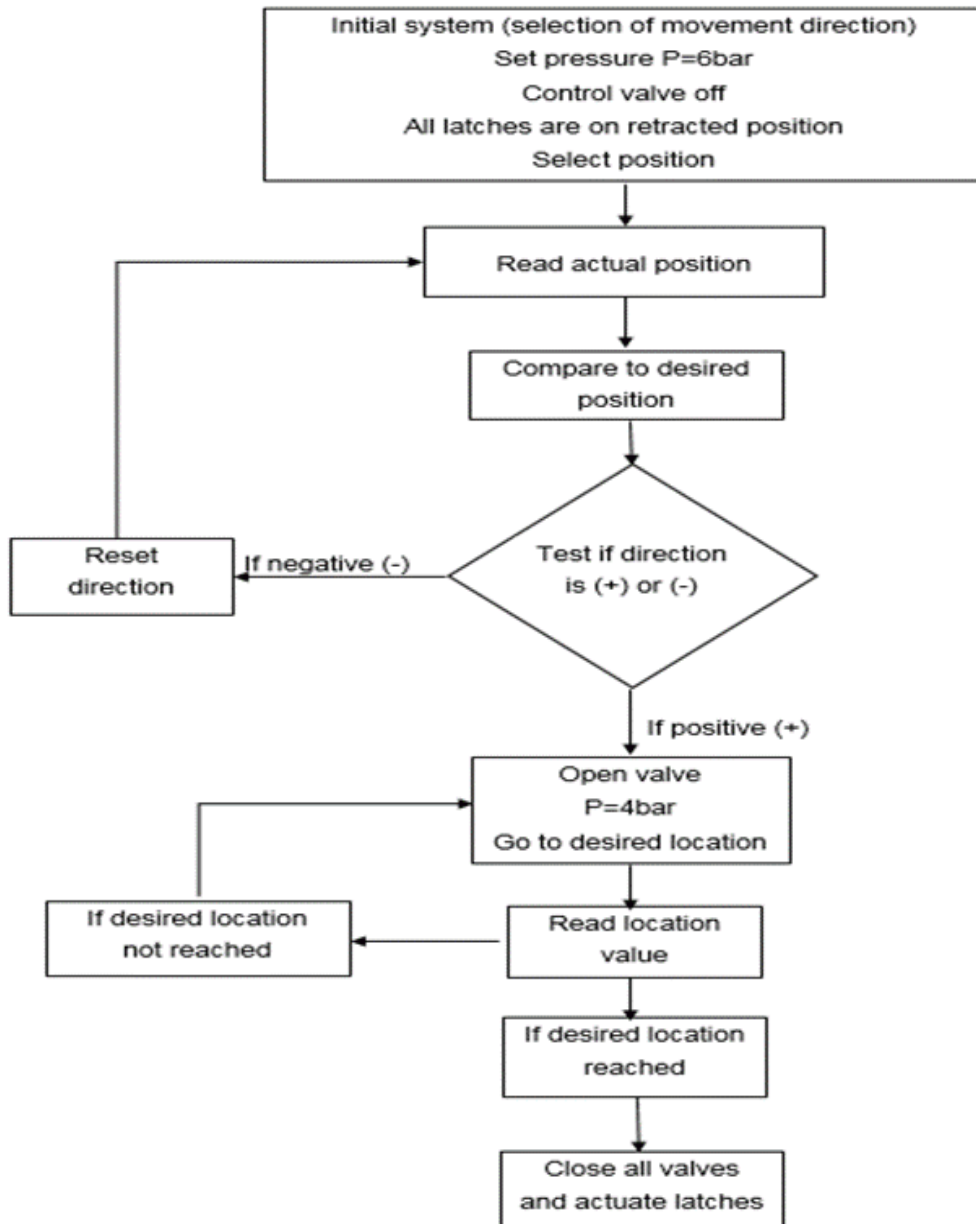


Figure 5.4: Control system flowchart.

K600 COLLIMATOR LADDER CONTROL

Collimator Ladder Position

Collimator Ladder in Motion

Auto Positioning

Move the collimator ladder by selecting one of the three predefined Positions. Then Press GO

4.615 mm ---- Top

124.996 mm -- Middle

245.378 mm --- Bottom

Collimator in Beam

Manual Positioning

Choose a specific collimator ladder endpoint. Then press GO

Collimator Ladder Position: mm

Motion Control and Error Indication

Stop

Soft Limits

GO

Motion Errors: Drive in idling state after Go command submitted!!!

Figure 5.5: Graphical interface for collimator positioning.

Figure 5.5 shows the monitor used in the data or control room to remotely control the positioning of three collimators on the beam centre namely, the top, middle and bottom circled in colour yellow. The numbers written in blue colour next to the collimator position represent the distance of the collimator position from the reference point. The reference point being the bottom limit switch which was set as the zero position when coding, meaning the top collimator is 4.615 mm away from the bottom reference limit switch.

As previously mentioned two limit switches are installed, with one at the top outmost position and the other at the bottom minimal position and this are installed to avoid overshooting when running the motor for positioning. There are two safety system in place namely the mechanical safety and software safety. The software safety is the most recommended because it helps avoid accidents where components can get damaged and in this study the limit switch together with software are used for safety. The motor always try push down when it starts to rotate and if the only safety system is mechanical it would results in damaged components and with software it allows a safety factor to accommodate the opposite rotation hence it was the most recommended for the study.

5.3 Test and Validation

The vacuum department at iThemba LABS was responsible for testing any leaks around welds and bolted areas, connecting pumps in areas that operate under vacuum in the vault. Figure 5.5 shows the chamber undergoing leak test after welding to ensure that there is no leaks around welds. The detector machine uses Helium to identify if there is any air escaping or entering through the welds. The machine picked up leak from the first test and the chamber had to be sent back to the welding bay to fix leaking areas. After the leaky areas were fixed the chamber went back for testing and it passed the tests on the second round and it was cleared to be installed or assembled in the vault.



Figure 5.6: Chamber leak testing.

After installation of the prototype at the K600 magnetic spectrometer, leak tests were run on the prototype and its connecting lines in the spectrometer. The most important test which had to be performed first was that of leak detection as it can cause automatic failure in any experimental study if leaking occurs. With the leak test results obtained from the spectrometer after installation, it was confirmed that the chamber is leak tight and is able to achieve the required vacuum.

The second test carried out was experimental tests performed by the client/end-user. The experimental physicist needed to run test on the model before performing main experiments to see if the new mechanism gives same results compared to the once obtained in the past using the old carousel. The reason for the results to be similar to those obtained in the past being that the collimators and beamstop shape did not change, the only change made was the driving mechanism and the chamber design.

Changing the drive mechanism was done to improve and provide safe working environment for employees as they will be using technology to remotely control the prototype operation. The collimator mechanism improves the results by making it possible to do experiment at any angle rather than being restricted to few angles like previously with the carousel. With the results, researchers obtained from the test conducted on the new prototype it can be confirmed that they were satisfied with the mechanism and it met all their requirements. Overall the model met the end-users requirements which were:

- To reduce radiation dose for staff,
- Efficient use of beamtime
- Preventing scattered particles from entering the K600 during beam tuning exercises,
- Less time needed for pre-experimental preparations.

CHAPTER 6

Conclusions and Recommendations

6.1 Conclusions

The aim of the study was to design and manufacture a collimator mechanism that operates at all angle modes of the K600 magnetic spectrometer at iThemba LABS. The components used to make the collimator mechanism (prototype) were successfully designed and manufactured at iThemba LABS mechanical workshop except the off-shelf ones. After assembly and installation of the prototype, vacuum test were performed to ensure that there are no leaks around sealed or bolted areas to avoid adding on to the pumping time if there is leaks. If there are any leaks time can be wasted because the pumping process would take longer than required hence leak tests were thoroughly done before the prototype could be pumped down.

Furthermore, experimental tests were performed in order to observe the results of the new collimator mechanism and compare them with the results obtained in the past using the old carousel in angle ranging between 6° - 360° . These results needed to be similar due to the fact that the experimental procedure being carried out is still the same to those carried out in the past; the only difference is the drive mechanism for positioning and the small angle mode coverage. The experimental results obtained were satisfactory as the end user was able to get accurate results at all angle modes of the k600 magnetic spectrometer.

From the output obtained during experimental tests, it can be concluded that designing remote controlled collimator mechanism was ideal for the system as the spectrometer can now function in all angle including small angle. It was per expected outcomes of the study which required the use of pneumatics drive to position collimators onto the beamline. The prototype was shown to be capable of performing at small angle modes of the spectrometer. The study proved a success as the prototype manufactured is able to reduce the loss of beamtime. Moreover, it is also safe to work with as the prototype is remotely controlled from the data room. There is less exposure to radiation for the employees as there is no manual collimator changes and alignment required during experiment process. Therefore the study met the outlined objectives and requirements.

6.2 Recommendations

There is a room for improvement in the future on the model design, material choice and sizes. The chamber body can be improved by using separate plates and weld them together to make a box rather than bending the u-shape plate and just close it up. Bending the u-shape can result in loss of squareness which can affect the welding process and the prototype as a whole. Welding with distorted material or material that is not square can be time-consuming as the welding procedure would take longer than required because one will be trying to ensure the squareness is achieved. Hence in the future it is best to use four separate plates which are easy to clamp to achieve the squareness compared to bending the plates.

In this project the collimator ladder required to be further back close to the quadrupole in order to achieve the small angle and have the beam stopping at the centre of the beamstop web. The reason for having the ladder further back is that the distance from the scattering chamber to the collimator and beamstop centre is limited. To achieve a small angle the distance needs to be at least 900mm. This distance can be improved in the future by using a different valve or by reducing the valve adaptor plate thickness and the flange going through the quadrupole. With this project we hope to achieve better experimental results for all angle modes of the k600 magnetic spectrometer.

BIBLIOGRAPHY

Adsley, P., Neveling, R., Papka, P., Dyers, Z., Brümmer, J.W., Diget, C.A., Hubbard, N.J., Li, K.C.W. et al. 2017. CAKE: The Coincidence Array for K600 Experiments, South Africa. 2:1-4.

Berg G.P.A., Foster C.C. & Stephenson E.J. 1993-1994. K600 Transmission mode for 0° inelastic scattering. Indiana University Cyclotron Facility: Bloomington, Indiana.

Budynas, R.G & Nisbett, J.K.2009. *Shigley's Mechanical Engineering Design*. 9th Ed. McGraw Hill. New York. 223.

Dalesio L.R. 1989. The ground test accelerator database: a generic instrumentation interface, in accelerator and large experimental physics control systems. British Columbia. Canada. 288-291.

de Vasconcelos D.A.A., Hamada M.M., Mesquita H.C., Dantals C.C., Narain R., Melo B.S. & dos Santos V.A. 2011. Collimator design for single beam gamma ray industrial tomography and fan beam geometry. International nuclear Atlantic conference. 24-28 October 2011. Federal University of Pernambuco. Brazil, Belo horizonte.

Drotsky, J.G. 2011. *Strength of materials for technicians*. 4th ed. Cape Town, South Africa: Parow Industria. 221-233.

Festo.2018. Directional control valves. Available: <http://www.festo-didactic.com>. [2018, March 2].

Fontana, M. 2005. *Computer simulation mathematics and economics*. Torino. Italy.

Jordan, T.J. & Williams, P.C. 1994. The design and performance characteristics of a multileaf collimator, *Phys.Med.Biol.* 39:231-251.

Kheswa, N.Y., Buthelezi, E.Z. & Lawrie, J.J. 2008. Making of targets for physics experiments at iThemba LABS. 590(1-3):114-117.DOI: 10.1016/j.nima.2008.02

Langro, F. 2011. Pneumatics vs electrics: a niche for each. 22 June. Available: <http://www.designworldonline.com/pneumatics-vs-electrics-a-niche-for-each/>. [2017, July 12].

Magdziak, L., Malujda, I., Wilczynski, D. & Wojtkowiak, D. 2016. "Concept of improving positioning of pneumatic drive as drive of manipulator", *Procedia Engineering* 177 (2017) 331 – 338. 21 International Slovak–Polish Conference. Poland.

Naude, P. 2017. *Practical finite element analysis [FEA101 Lecture notes]*. ESTEQ Institute of Technology.

Neveling, R., Smit, F.D., Fujita, H. & Newman, R.T. 2008. *K600 user manual*, iThemba LABS, Somerset west. Unpublished.

Neveling, R., Smit, F.D., Fujita, H., Adsley, P., Li, K.C.W., Brümmer, J.W., Marin-Lambarri, D.J. & Newman, R.T. 2017. *Guide to the K600 magnetic spectrometer*.

Philipfigari. 2015. Steps to /strain analysing a material's properties from its stress curve. Available: <http://www.instructables.com/id/Steps-to-Analyzing-a-Materials-Properties-from-its/> [2018, March 15].

RS Components. 2018. Available: <https://za.rs-online.com/web/op/all-products/> [2018, March 2].

Sedcole, P. 2008. *Latches & Flip-flops digital electronics 1*. [Lecture9]. Imperial College London.

Shailendra, K.B., Prakash, K.S. & Vivek, M. 2015. *Virtual manufacturing and their application*. *International Journal for Research in Applied Science & Engineering Technology (IJRASET)*. 3 (V): 350-352.

Shirazu, I., Amuasi, J. H., Boadu, M., Sosu, E. K. & Hasford, F. 2013. *The Effect of Collimator Selection on Acquisition Time with varying Acquisition Parameters using Quadrant Bar Phantom at Korle-Bu Teaching Hospital*. Accra, Ghana. 3(5): 277-280. Available: <http://www.ejournalofsciences.org> [2017, June 28].

Sorenson, J.A. & Phelps, M.E. 1987. *Physics in nuclear medicine*. 2nd ed. Philadelphia. WB Saunders Company. 16: 331-345.

Usman, I.T. 2009. *Fragmentation of the isoscalar giant quadrupole resonance in low mass $12 \leq A \leq 40$ nuclei and 2^+ level density in ^{40}Ca from high energy-resolution (p,p') scattering at 200 MeV*. Ph.D. Thesis. University of the Witwatersrand.

Van Hagan, T.H., Doll, D.W., Schneider, J.D. & Spinos, F.R. 1998. *Design of an Ogive-shaped beamstop*. *proc LINAC98*. Chicago (618-620).

Womack. 1990. Fluid power design data sheet. Womack educational publication.
<http://www.womack-educational.com>. [2018, March 2].

Wronka, S. 2011. High power hadron machines, CAS Bilbao, 1-19.

APPENDICES

APPENDIX A

Detailed drawings of the three collimators

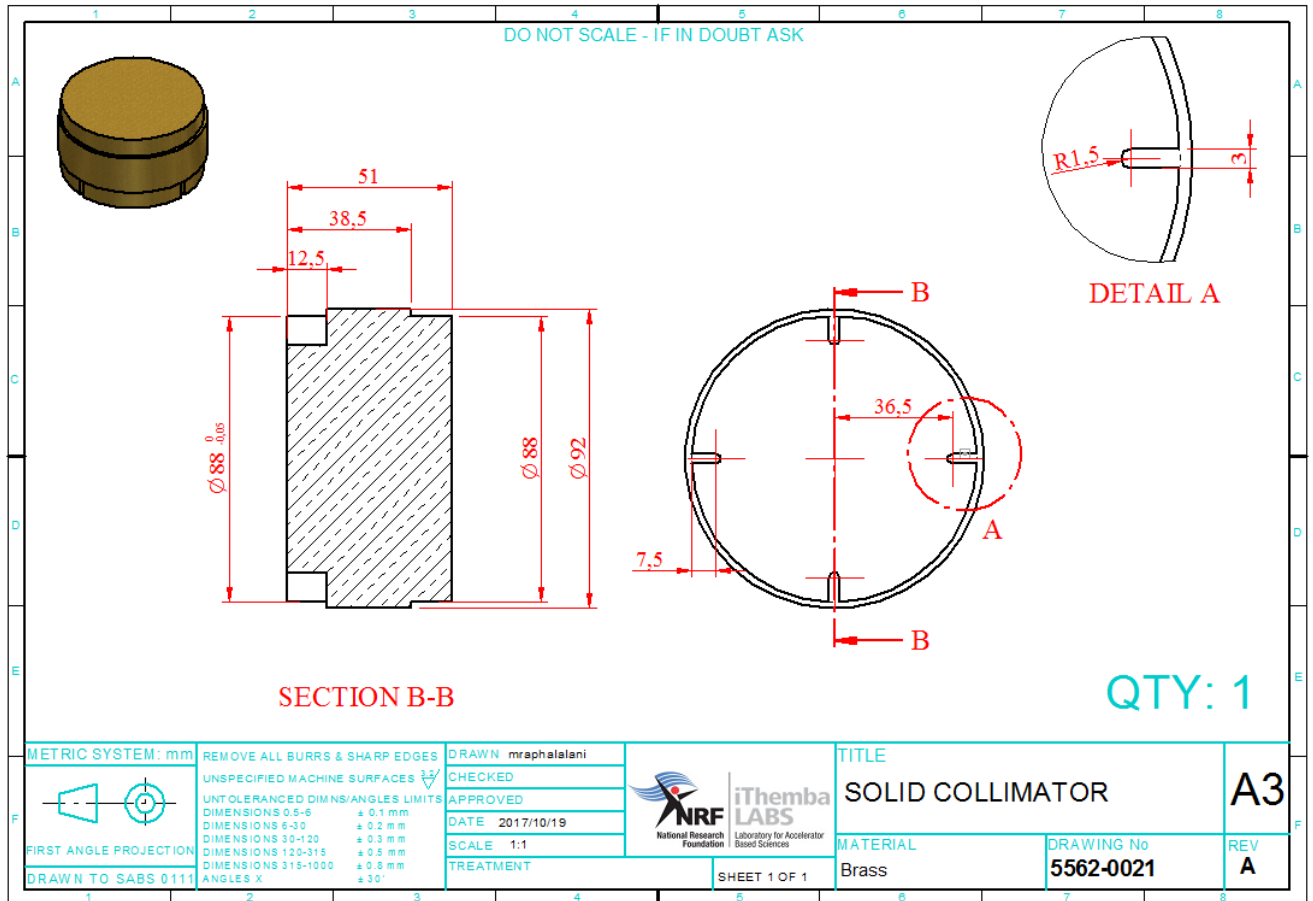


Figure A.1: Solid collimator

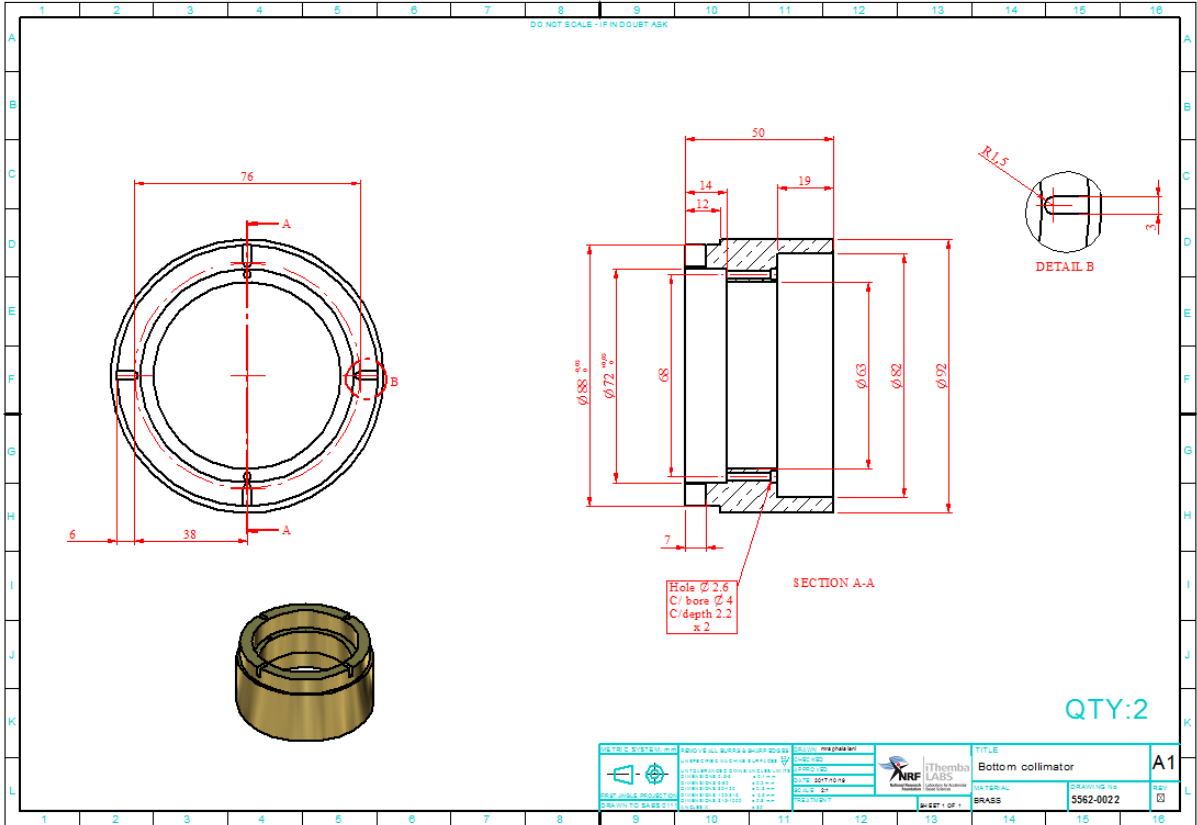


Figure A.2: Collimator accommodating inserts

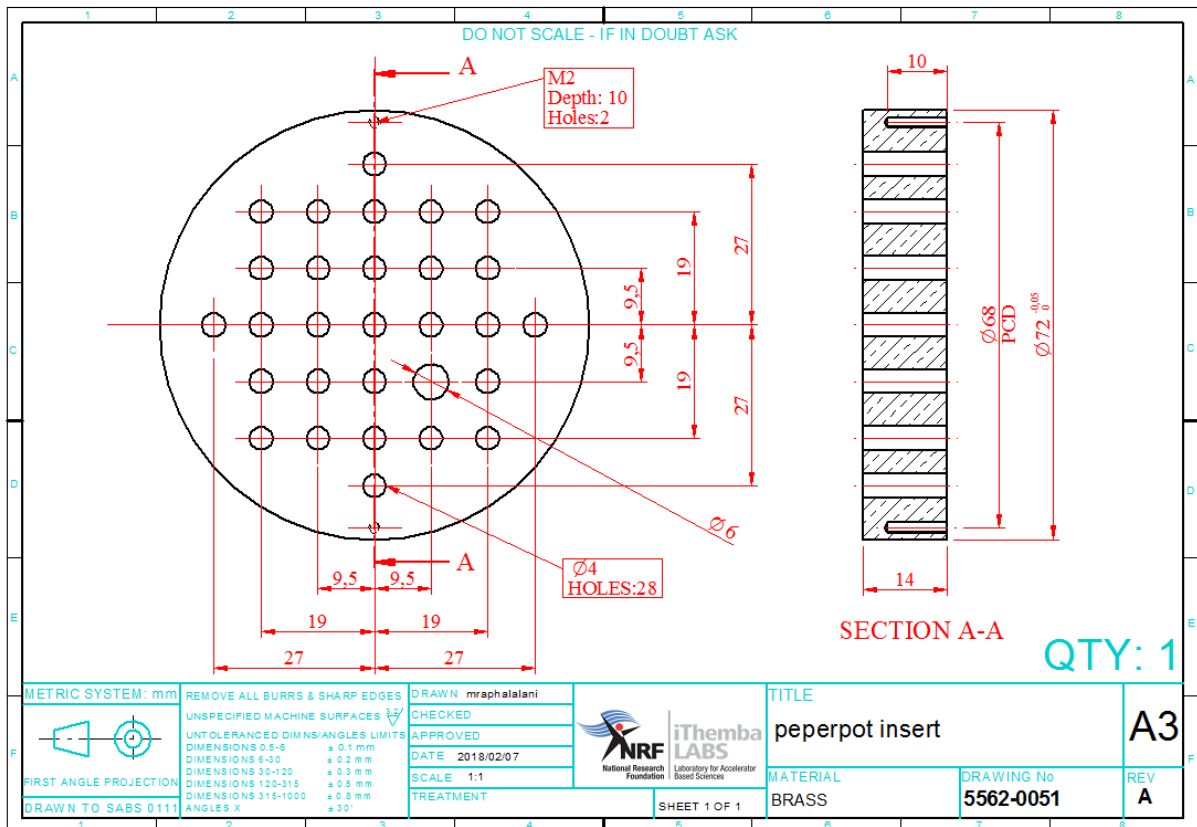


Figure A.3: Peperpot insert

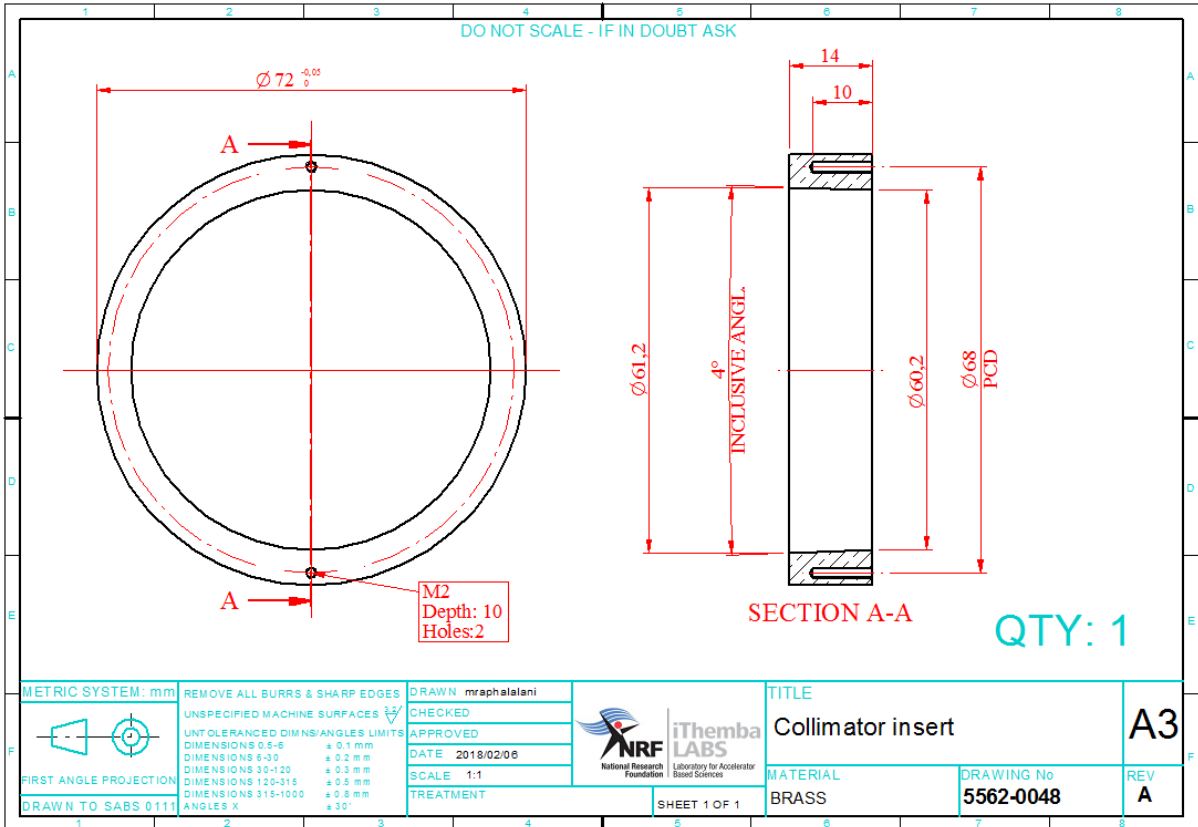


Figure A.4: Angular insert.

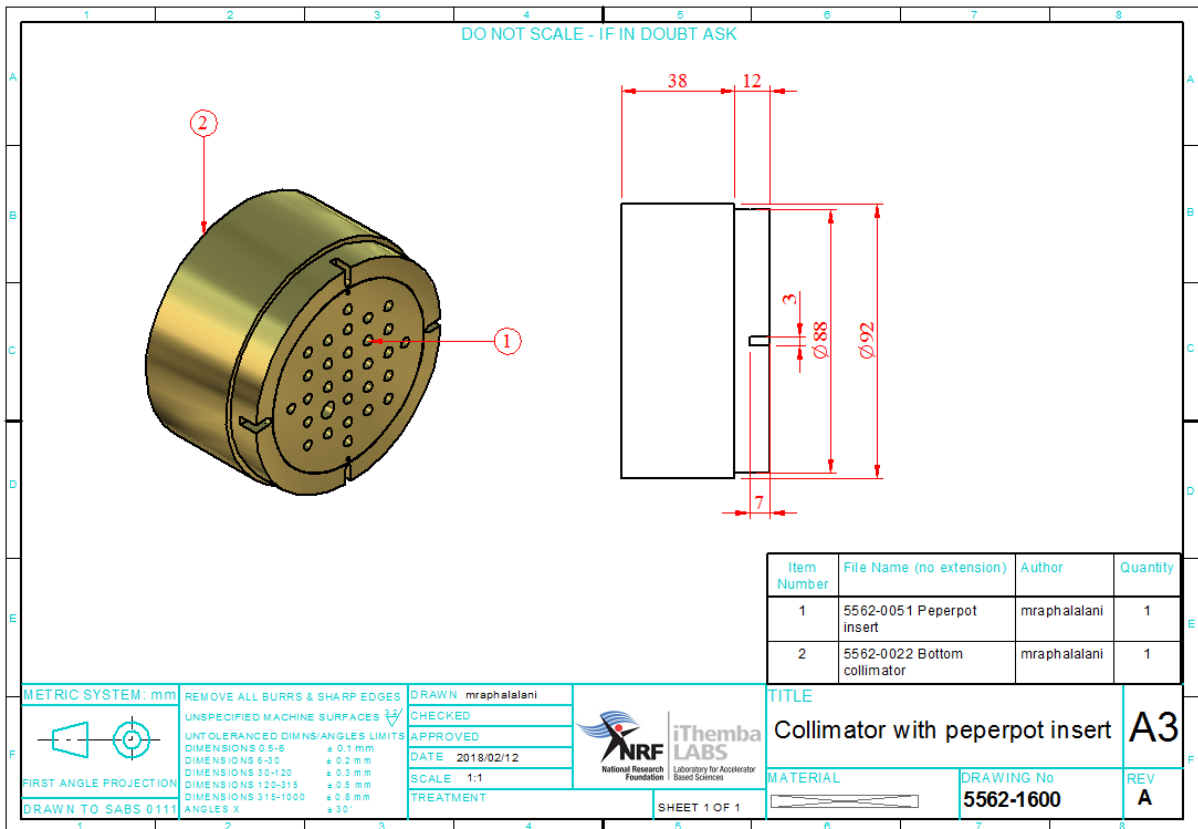


Figure A.5: Collimator with peperpot insert assembly.

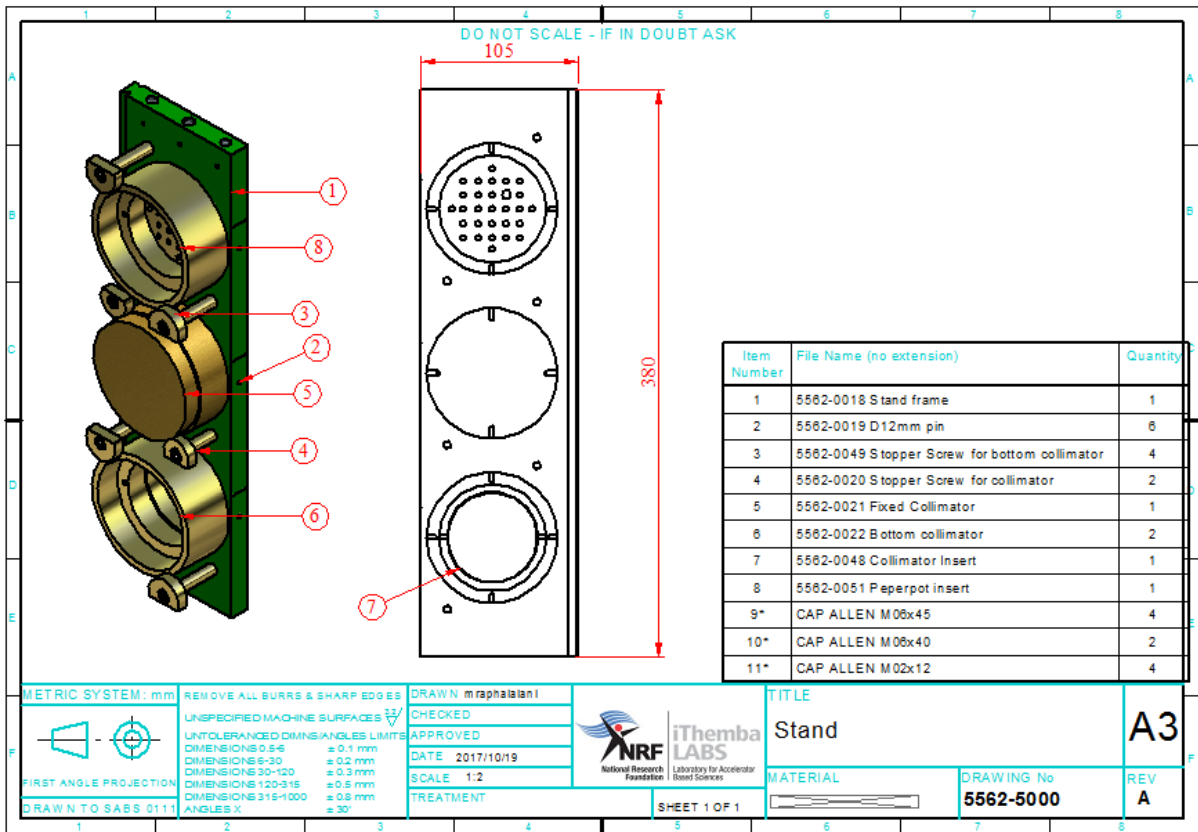


Figure A.6: Three collimators assembled to the ladder

APPENDIX B

Overall detailed design of the prototype

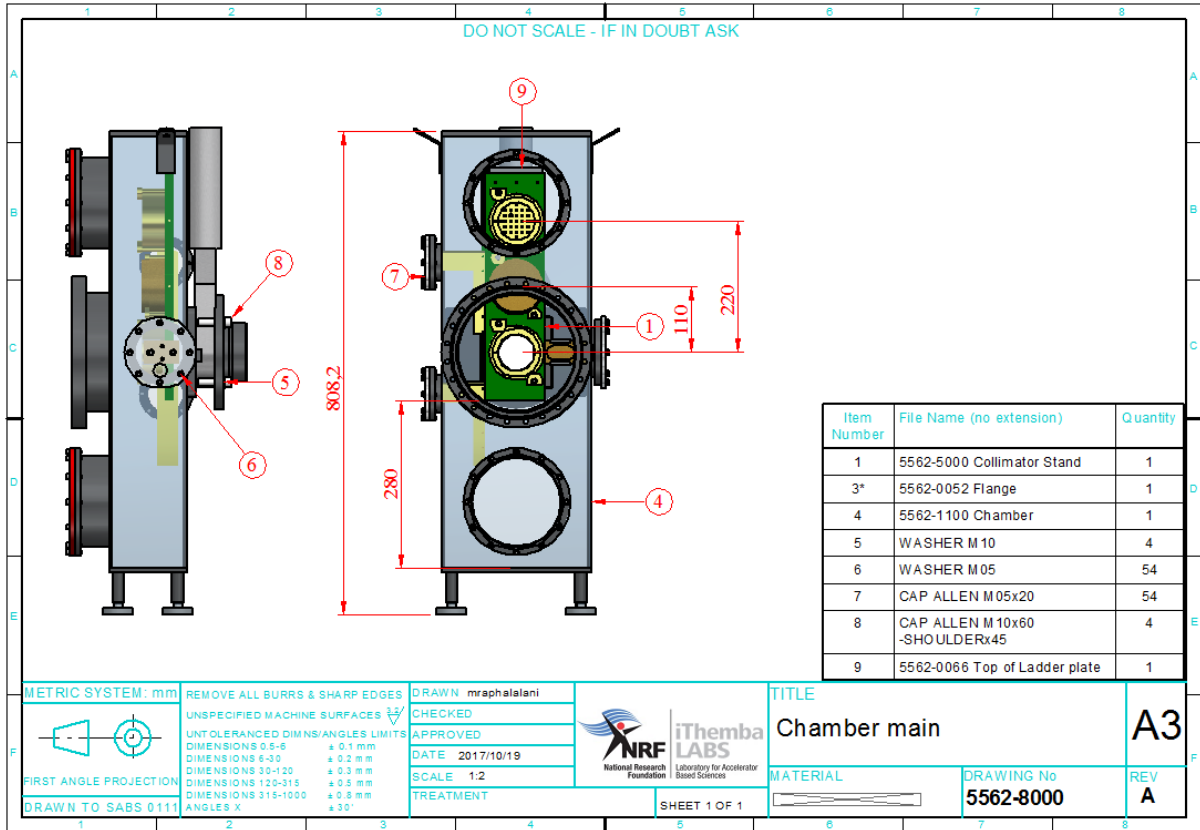


Figure B.1: Chamber assembly

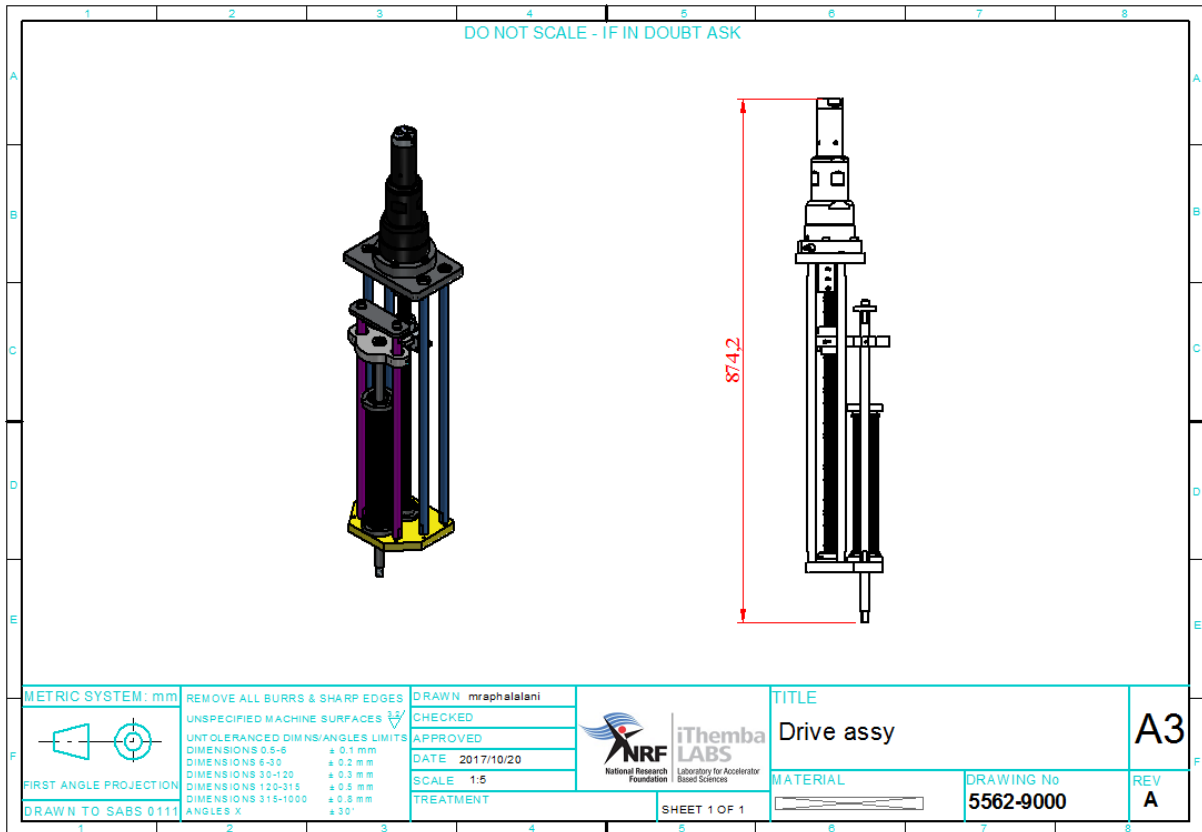


Figure B.2: Top level assembly driving the motor

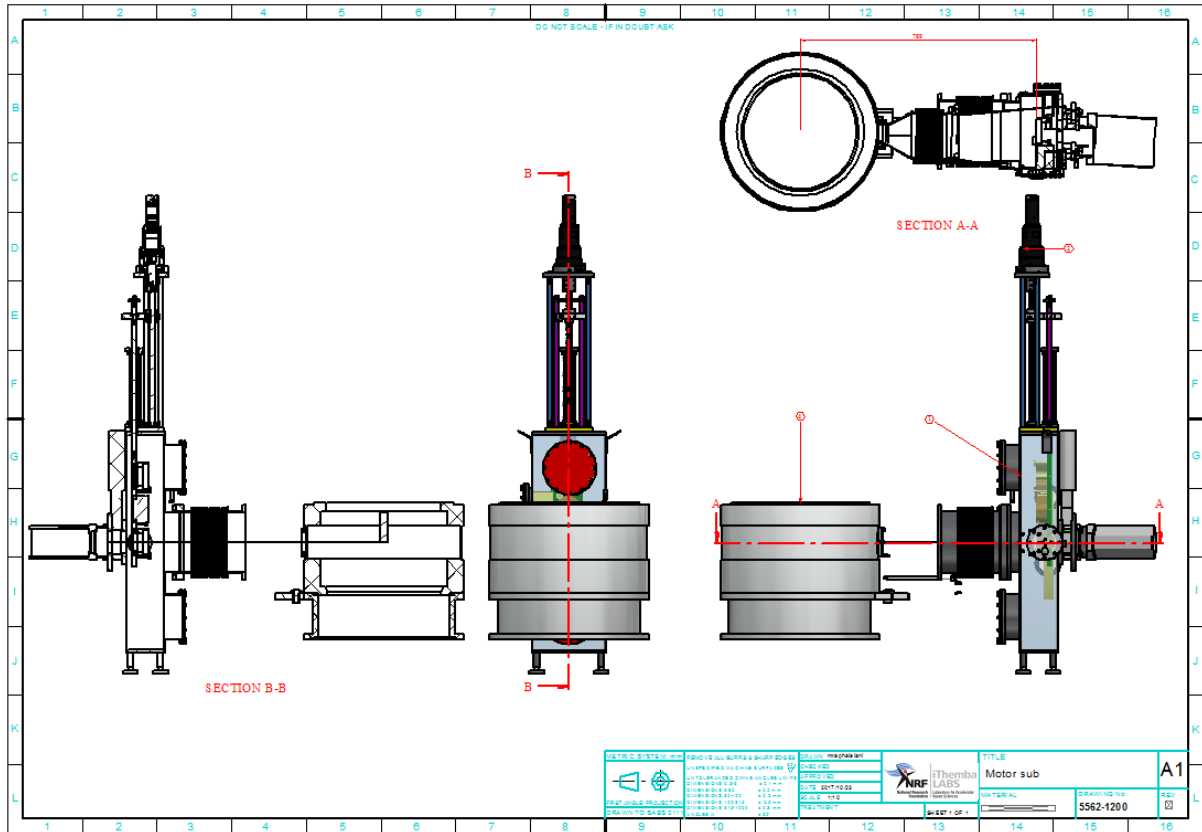


Figure B.3: The prototype assembled with the sliding seal scattering chamber.

APPENDIX C

Epics Substitution file

```
## Load the master bus template file##
file "db/MASTER.template" {

    pattern { SYS      DEVICE    PORT      SCAN    }
             { SAMVC    MASTER    MASTER0   "I/O Intr"    }
}
## Load the bus coupler template file###
file "db/EK1100.template" {

    pattern { SYS      DEVICE    PORT      SCAN    }
             { SAMVC    COUPLER   ERIO.0    "I/O Intr"    }
}
#####
####
# Load the bus Inputs template files
# Field Input Interface to Beckhoff Modules ###
# The field output interface is done via 10 Beckhoff output
modules(EL1862)
#####
file "db/EL3255.template" {

pattern
  { SYS      DEVICE    SCAN      PORT      INPUT1     INPUT2
INPUT3     INPUT4     INPUT5     INPUT6     INPUT7     INPUT8   }
  {"SAMVC"   "AIM1"    "I/O Intr" ERIO.1     TARPOFSB   INU1
INU2       INU3       INU4       INU5       INU6       INU7     }
}

file "db/EL4004.template" {
pattern
  {      SYS      DEVICE    SCAN      PORT
OUTPUT1     OUTPUT2     OUTPUT3     OUTPUT4 }
  {"SAMVC"   "AOM1"    "Passive" ERIO.2   PDCVSETP:RAW PPRSETP:RAW
ONU1
ONU2       }
}

file "db/EL2808.template" {
pattern {
  SYS      DEVICE    SCAN      PORT      OUTPUT1     OUTPUT2
OUTPUT3     OUTPUT4     OUTPUT5     OUTPUT6     OUTPUT7     OUTPUT8   }
  {"SAMVC"   "DOM1"    "Passive" ERIO.3   TARPOSLACTH:1 TARPOSLACTH:2
TARPOSLACTH:3 ONU1     ONU2     ONU3     ONU4     ONU5     }
}

file "db/EL1808.template" {
pattern {
  SYS      DEVICE    SCAN      PORT      INPUT1     INPUT2
INPUT3     INPUT4     INPUT5     INPUT6     INPUT7     INPUT8
}
  {"SAMVC"   "DIM1"    "I/O Intr" ERIO.4   CL1LIM-OUT CL1LIM-IN INU1
INU2       INU3       INU4       INU5     INU5     }
}
#####
###
```

```

# load Ebus Template: Ensure the operating status of Bus devices
#####
##
file "db/ebus-monitor.template" {
    {
        SYS                                = "SAMVC"
        scan                               = ".1 second"
        on                                  = 1
        off                                  = 0
    }
}
#####
# digital full scale = 32768 (15 bits)
# analog full scale = 10 V
# targDispFS is the working range from top to bottom
# mmCal represent the mm offset from the absolute origin here the pot
surface(actual 0 reading on pot)
# potcal represent the pot count at mmCal or the pot offset from
absolute 0
# potCntPerMm = potCntFS / targFSMm # this include an offset.
# the flow rate is describe by the PDCV percentage opening[0-100%]/[0-
1] in both direction
# the opening range is from [0 - 4.5V ] CW and [5.5 - 10 V] one need to
measure the actual value
# pdcvOpperCnts = pdcvDownMax(counts) / 100 (%)
#####
#####
file "db/iocsamvc-pot.template" {
    {
        SYS                                = "SAMVC"
        PV                                  = "TARPOFB:RAW"
        scan                               = ".01 second"
        lnPotPerMm = 108.957#99.683 # (counts/mm) # may need
recalculation when limits are installed
        calMin = 1546 # beyond target Top
must be fix reference
        calMax = 26606
        mmCal = 0 # mm
        targFS = 25060
        targFSMm = 230 # mm
        mmMax = 232 # mm
        mmMin = 0
    }
}
### After motor stop(from pos reached one still need to compare the
actual position to the wanted one
### when hitting a limit the reverse works: one may add a timer to
reverse and stop
file "db/iocsamvc_inprogress.template" {
    {
        SYS                                = "SAMVC"
        ppr                                  = "PPRSETP:RAW"
        pdcv                                  = "PDCVSETP:RAW"
        limIn = "CL1LIM-IN"
        limOut = "CL1LIM-OUT"
        scan                                  = ".01 second"
        startTimer = ".01 second"
        stopTimer = "Passive"
    }
}

```

```

startRevTimer      = ".1 second"
stopRevTimer       = "Passive"
topCnts            = 2060          # old: 2100      # counts

topMm              = 4.717         #5.216 # 2060      # 25.776
midCnts            = 14045         #14050      # 14054 old readings
middleMm           = 114.715      #125.538    # 135.776
#135.158 mm absolute scale
botCnts            = 26030         #26000
bottomMm           = 224.712      #245.378    # 245.158
absolute scale
softLmtOut         = 3.717         # mm or 2660 eng
# beyond target Top
softLmtIn          = 225.712      # mm or beyond target
Bottom
hardLmtin          = 26606         # beyond target
Bottom must be fix reference
hardLmtout         = 1546         # beyond target
Bottom must be fix reference
pdcvOff            = 16384         # valve in middle
position(fully closed) # need to measure analog full scale and get the
cnts corresponding
pdcvOpperCnts     = 163.84         #( counts / % opening)
pprOff             = 0             # counts ~ 0 bars
pprInitP           = 2000         # counts
pprMaxP            = 10000        # counts
pprlnrCnst         = 0.0342       # Linearization cnst
pprlnrSlp          = 0.00015     # Linearization slope : accuracy of
output pressure is not a constraint we just need to be close
pdcvCWOn           = 0            # 1-->2(fully open)
pdcvCCWOn          = 32000        # 1-->4(fully open)

pdcvIntUp          = 50           # % opening starting
from 50%
pdcvIntDown        = 0.0         # % opening starting from
0 %
pdcvDownMax        = 16384        # hardware meaure need to
confirm exact value: by measure full scale(voltage)
pdcvUpmax          = 32000        # hardware meaure need to
confirm exact value: by measure full scale(voltage)
emStartCnt         = 100          # ~2 second(test the
travel distance at init pressure after 1 second)
revStartCnt        = 100          # ~2 second(test the
travel distance at init pressure after 1 second)
emMinDisp          = 0.1          # 5 mm ~ 533 cnts
on                  = 1
off                 = 0
lnk1                = 1
lnk2                = 2
lnk3                = 3
potNoise           = 0.035 # mm ( max expected noise on pot
input)
mmMax              = 232          # mm
mmMin              = 0
}
}

```

Epics IOC data base template

```
## Load the master bus template file##
file "db/MASTER.template" {

    pattern { SYS      DEVICE    PORT      SCAN      }
             { SAMVC    MASTER    MASTER0   "I/O Intr" }
}
## Load the bus coupler template file###
file "db/EK1100.template" {

    pattern { SYS      DEVICE    PORT      SCAN      }
             { SAMVC    COUPLER   ERIO.0    "I/O Intr" }
}
#####
####
# Load the bus Inputs template files
# Field Input Interface to Beckhoff Modules ###
# The field output interface is done via 10 Beckhoff output
modules(EL1862)
#####
file "db/EL3255.template" {

pattern
  { SYS      DEVICE    SCAN      PORT      INPUT1     INPUT2
INPUT3  INPUT4     INPUT5     INPUT6     INPUT7     INPUT8     }
  {"SAMVC"   "AIM1"     "I/O Intr" ERIO.1     TARPOFB    INU1
INU2     INU3       INU4       INU5       INU6       INU7       }
}

file "db/EL4004.template" {
pattern
  {      SYS      DEVICE    SCAN      PORT
OUTPUT1     OUTPUT2     OUTPUT3     OUTPUT4 }
  {"SAMVC"   "AOM1"     "Passive" ERIO.2   PDCVSETP:RAW PPRSETP:RAW
ONU1
ONU2     }
}

file "db/EL2808.template" {
pattern {
  SYS      DEVICE    SCAN      PORT      OUTPUT1     OUTPUT2
OUTPUT3     OUTPUT4     OUTPUT5     OUTPUT6     OUTPUT7     OUTPUT8     }
  {"SAMVC"   "DOM1"     "Passive" ERIO.3   TARPOSLACTH:1 TARPOSLACTH:2
TARPOSLACTH:3 ONU1     ONU2     ONU3     ONU4     ONU5     }
}

file "db/EL1808.template" {
pattern {
  SYS      DEVICE    SCAN      PORT      INPUT1     INPUT2
INPUT3     INPUT4     INPUT5     INPUT6     INPUT7     INPUT8     }
  {"SAMVC"   "DIM1"     "I/O Intr" ERIO.4   CL1LIM-OUT CL1LIM-IN INU1
INU2     INU3     INU4     INU5     INU5     }
}
#####
####
# load Ebus Template: Ensure the operating staus of Bus devices
```

```

#####
##
file "db/ebus-monitor.template" {
    {
        SYS                                = "SAMVC"
            scan                            = ".1 second"
            on                               = 1
            off                              = 0
    }
}
#####
# digital full scale = 32768 (15 bits)
# analog full scale = 10 V
# targDispFS is the working range from top to bottom
# mmCal represent the mm offset from the absolute origin here the pot
surface(actual 0 reading on pot)
# potcal represent the pot count at mmCal or the pot offset from
absolute 0
# potCntPerMm = potCntFS / targFSMm # this include an offset.
# the flow rate is descibe by the PDCV percentage opening[0-100%]/[0-
1] in both direction
# the opening range is from [0 - 4.5V ] CW and [5.5 - 10 V] one need to
measure the actual value
# pdcvOpperCnts = pdcvDownMax(counts) / 100 (%)
#####
#####
file "db/iocsamvc-pot.template" {
    {
        SYS                                = "SAMVC"
            PV                               = "TARPOFB:RAW"
            scan                              = ".01 second"
            lnPotPerMm = 108.957#99.683 # (counts/mm) # may need
recalculation when limits are installed
            calMin = 1546 # beyond target Top
must be fix reference
            calMax = 26606
            mmCal = 0 # mm
            targFS = 25060
            targFSMm = 230 # mm
            mmMax = 232 # mm
            mmMin = 0
    }
}
### After motor stop(from pos reached one still need to compare the
actual position to the wanted one
### when hitting a limit the reverse works: one may add a timer to
reverse and stop
file "db/iocsamvc_inprogress.template" {
    {
        SYS                                = "SAMVC"
            ppr                               = "PPRSETP:RAW"
            pdcv                              = "PDCVSETP:RAW"
            limIn = "CL1LIM-IN"
            limOut = "CL1LIM-OUT"
            scan                              = ".01 second"
            startTimer = ".01 second"
            stopTimer = "Passive"
            startRevTimer = ".1 second"
    }
}

```

```

        stopRevTimer      =      "Passive"
        topCnts           = 2060          # old: 2100      # counts

        topMm            = 4.717          #5.216 # 2060      # 25.776
        midCnts          = 14045          #14050      # 14054 old readings
        middleMm         = 114.715       #125.538    # 135.776
#135.158 mm absolute scale
        botCnts          = 26030          #26000
        bottomMm         = 224.712       #245.378    # 245.158
absolute scale
        softLmtOut      = 3.717          # mm or 2660 eng
        # beyond target Top
        softLmtIn       = 225.712       # mm or beyond target
Bottom
        hardLmtin      = 26606           # beyond target
Bottom must be fix reference
        hardLmtout     = 1546           # beyond target
Bottom must be fix reference
        pdcvOff        = 16384          # valve in middle
position(fully closed) # need to measure analog full scale and get the
cnts corresponding
        pdcvOpperCnts = 163.84         #( counts / % opening)
        pprOff         = 0              # counts ~ 0 bars
        #!../../bin/linux-x86_64/iocsamvc

## You may have to change iocvcs to something else
## everywhere it appears in this file

< envPaths

cd "${TOP}"

## Register all support components
dbLoadDatabase "dbd/iocsamvc.dbd"
iocsamvc_registerRecordDeviceDriver pdbbase

## Load record instances
ecAsynInit("/tmp/scan1", 1000000)

#dbLoadTemplate "db/iocsamvc.substitutions"
dbLoadTemplate "db/iocsamvc_inprogress.substitutions"

## Set this to see messages from mySub
#var mySubDebug 1

## Run this to trace the stages of iocInit
#traceIocInit

#autosave:
set_savefile_path("../save")
set_pass0_restoreFile("iocsamvc.sav")
set_pass1_restoreFile("iocsamvc.sav")
save_restoreSet_RetrySeconds(120)
set_requestfile_path( "./")
cd "${TOP}/iocBoot/${IOC}"
iocInit

```

```

create_monitor_set("iocsamvc.req",300)

## Start any sequence programs

    pprInitP      = 2000                # counts
    pprMaxP      = 10000               # counts
    pprlnrCnst   = 0.0342              # Linearization cnst
    pprlnrSlp    = 0.00015            # Linearization slope : accuracy of
output pressure is not a constraint we just need to be close
    pdcvCWOn     = 0                   # 1-->2(fully open)

    pdcvCCWOn    = 32000              # 1-->4(fully open)

    pdcvIntUp    = 50                  # % opening starting
from 50%
    pdcvIntDown  = 0.0                 # % opening starting from
0 %
    pdcvDownMax  =16384                # hardware measure need to
confirm exact value: by measure full scale(voltage)
    pdcvUpmax    =32000                # hardware measure need to
confirm exact value: by measure full scale(voltage)
    emStartCnt   = 100                 # ~2 second(test the
travel distance at init pressure after 1 second)
    revStartCnt  = 100                 # ~2 second(test the
travel distance at init pressure after 1 second)
    emMinDisp    = 0.1                 # 5 mm ~ 533 cnts
    on           = 1
    off          = 0
    lnk1         = 1
    lnk2         = 2
    lnk3         = 3
    potNoise     = 0.035 # mm ( max expected noise on pot
input)
    mmMax        = 232                 # mm
    mmMin        = 0
}
}

```


Epics IOC execution template

```
#####
# Auto Mode: start by reading back the intended destination
#Read back user Selected Position
#####
record(seq, "$(SYS):Top-Sel")
{
    field(PINI,"YES")
    field(DOL1,"$(topMm)")
    field(DOL2,"$(on)")
    field(LNK1,"$(SYS):Put-P PP")
    field(LNK2,"$(SYS):Put-Auto PP")
    field(SELM,"All")
}
record(seq, "$(SYS):Mid-Sel")
{
    field(PINI,"YES")
    field(DOL1,"$(middleMm)")
    field(DOL2,"$(on)")
    field(LNK1,"$(SYS):Put-P PP")
    field(LNK2,"$(SYS):Put-Auto PP")
    field(SELM,"All")
}
record(seq, "$(SYS):Bot-Sel")
{
    field(PINI,"YES")
    field(DOL1,"$(bottomMm)")
    field(DOL2,"$(on)")
    field(LNK1,"$(SYS):Put-P PP")
    field(LNK2,"$(SYS):Put-Auto PP")
    field(SELM,"All")
}
record(ao,"$(SYS):Put-P")
{
    field(DTYP,"Soft Channel")
    #field(VAL, "$(middleMm)")
    field(PINI,"YES")
    field(HOPR, "$(mmMax)")
    field(LOPR, "$(mmMin)")
    field(PREC,"3") # 3 decimal point
    field(EGU,"mm") #
    field(FLNK,"$(SYS):Init-M")
    info(autosaveFields_pass0, "VAL")
}
record(ao,"$(SYS):Get-InitP")
{
    field(DTYP,"Soft Channel")
    field(PINI,"YES")
    field(VAL, "$(middleMm)")
    field(OMSL,"closed_loop")
    field(DOL,"$(SYS):Get-P.VAL NPP")
    field(HOPR, "$(mmMax)")
    field(LOPR, "$(mmMin)")
    field(PREC,"3") # 3 decimal point
    field(EGU,"mm") #
    info(autosaveFields_pass0, "VAL")
}
```

```

}

record(ao, "$(SYS):Put-OutPp")
{
  field(DTYP, "Soft Channel")
  field(PINI, "YES")
  field(FLNK, "$(SYS):Put-PrsEng")
  field(VAL, "$(pprInitP)")
  info(autosaveFields_pass0, "VAL")
}
#####
# Init Motion:
# 1. Confirm a selection was made
# 2. Check interlocks
#####
record(seq, "$(SYS):Init-M")
{
  field(SCAN, "Passive")
  field(SELM, "All")
  field(DOL1, "$(on)")
  field(DOL2, "$(on)")
  field(LNK1, "$(SYS):P-Selected PP")
  field(LNK2, "$(SYS):Check-Interlocks.PROC PP")
}
#####
# Motion start interlocks include:
# 1. EtherCAT Ebus status
# 2. Oprator dirve actiavtion routine
# Reset drive if activated otherwise init control valve
#####
record(calc, "$(SYS):Check-Interlocks") {
  field(SCAN, "Passive")
  field(FLNK, "$(SYS):Interlocks-Status")
  field(CALC, "A?$(lnk1):$(lnk2)")
  field(INPA, "$(SYS):Motion-Interlocks PP")
}
record(calc, "$(SYS):Motion-Interlocks") {
  field(SCAN, "Passive")
  field(CALC, "A||B?$(on):$(off)")
  field(INPA, "$(SYS):Soft-Interlocks PP")
  field(INPB, "$(SYS):EtherCAT-Interlocks NPP")
}
#####
# Check for soft Interlocks
# Put drive in idle state when activated
# Soft error can only happen after a position was selected
# Meaning after a positionis choosen they must clear
# maybe emergency start should not be included here
#####
record(calcout, "$(SYS):Soft-Interlocks") {
  field(SCAN, "Passive")
  #field(PINI, "YES")
  field(CALC, "A||B||C?$(on):$(off)")
  field(INPA, "$(SYS):Put-Abort.VAL NPP")
  field(INPB, "$(SYS):Em-Stop NPP")
  field(INPC, "$(SYS):Put-Org NPP")
  field(OUT, "$(SYS):Soft-IntlksError PP")
}

```

```

#####
# Reset drive when interlocks are active
# otherwise init control valve parameters
#####
record(fanout, "$(SYS):Interlocks-Status") {
    field(SCAN, "Passive")
    field(SELM, "Specified")
    field(SELL, "$(SYS):Check-Interlocks NPP")
    field(LNK1, "$(SYS):Stop-Motion PP")
    field(LNK2, "$(SYS):Init-PprPdcv PP")
}
#####
# No Initial Interlocks: Intialise Contro valves for motion
#####
record(fanout, "$(SYS):Init-PprPdcv") {
    field(SCAN, "Passive")
    field(LNK1, "$(SYS):Put-D PP")
    field(LNK2, "$(SYS):Put-PrsEng PP")
    field(SELM, "All")
}
#####
#####
# Determine the direction of movement: Compute the flow % opening
# Get-P is greater than Put-P thus we move down(flow rate value from 0
- 15000)
# [0 - 100%] [ 0 - 16384] downward : [0 - 100%] [ 16384 - 32768]
upwards
#####
#####
record(calc, "$(SYS):Put-D") {
    field(SCAN, "Passive")
    field(PINI, "YES")
    field(FLNK, "$(SYS):Selected-D")
    #field(CALC,
"B>A?$(pdcvIntDown)*$(pdcvOppperCnts):$(pdcvIntUp)*$(pdcvOppperCnts)+$(pdcvDownMax) ")
    field(CALC,
"C?$(pdcvIntDown)*$(pdcvOppperCnts):D?$(pdcvIntUp)*$(pdcvOppperCnts)+$(pdcvDownMax):B-
A>=0?$(pdcvIntDown)*$(pdcvOppperCnts):$(pdcvIntUp)*$(pdcvOppperCnts)+$(pdcvDownMax) ")
    field(INPA, "$(SYS):Put-P NPP")
    field(INPB, "$(SYS):Get-P NPP")
    field(INPC, "$(SYS):LmtIn-Act NPP")
    field(INPD, "$(SYS):LmtOut-Act NPP")
    info(autosaveFields_pass0, "VAL")
}
#####
#####
# We need to remember the last direction of movement
# in order to protect against user selected other direction while in
motion
# we need to process this record only after go was pressed.
#####
#####
record(ao, "$(SYS):Put-OldD")
{
    field(DTYP, "Soft Channel")
}

```

```

        field(PINI,"YES")
    field(OMSL,"closed_loop")
    field(DOL,"$(SYS):Put-D NPP")
        info(autosaveFields_pass0, "VAL")
}
record(calc, "$(SYS):Selected-D") {
    field(SCAN, "Passive")
    #field(PINI, "YES")
    field(CALC, "0")
    field(INPA, "$(SYS):Put-D NPP")
        info(autosaveFields_pass0, "VAL")
}

#####
# Keep pressure under acceptable limits
# Set Default pressure otherwise
#####
record(calc,"$(SYS):Put-PrsEng")
{
    field(SCAN, "Passive")
    #field(PINI, "YES")
    field(CALC, "A>=$(pprOff) &&A<=$(pprMaxP) ?A:$(pprInitP)")
    field(INPA, "$(SYS):Put-OutPp NPP")
        info(autosaveFields_pass0, "VAL")
}
#####
# To initiate Motion :
# 1. We need a "position P to be selected"
# 2. The Motor to be in "idle state": Not in motion
# 3. The Go signal to be activated
# 4. we need to do a reverse-foward or forward-reverse movement
#####
record(bo,"$(SYS):Put-Go")
{
    field(SCAN, "Passive")
        field(FLNK,"$(SYS):Start-Motion")
    field(PINI, "YES")
    field(ZNAM, "OFF")
    field(ONAM, "ON")
    field(VAL, "0")
}
record(calcout,"$(SYS):Start-Motion")
{
    field(SCAN, "Passive")
    #field(PINI, "YES")
    field(CALC, "A&&!B&&!C&&D?$(on):$(off)")
    field(INPA, "$(SYS):P-Selected NPP")
    field(INPB, "$(SYS):Motion-Interlocks PP")
    field(INPC, "$(SYS):Drive-State NPP")
    field(INPD, "$(SYS):Put-Go NPP")
    field(OUT, "$(SYS):Goto-P.PROC PP")
    field(OOPT, "Transition To Non-zero")
    info(autosaveFields_pass0, "VAL")
}

#####
# we may need to open pressure regular with delay
# before opening control valve

```

```

# Emergency start will handle that
# Drive-State must only be updated after motion was confirm started
#####
record(seq, "$(SYS):Goto-P") {
  field(SCAN, "Passive")
  field(DOL1, "$(SYS):Get-P.VAL")
  field(DOL2, "$(SYS):Put-D.VAL NPP")# Best to reprocess this record
before using VAL
  field(DOL3, "$(SYS):Put-PrsEng.VAL NPP")# Best to reprocess this
record before using VAL
  field(DOL4, "$(on)")
  field(DOL5, "$(on)")
  field(DOL6, "$(on)")
  field(DOL7, "$(on)")
  field(DLY2, "0.1") # Get Init position before any movement on drive
  field(DLY3, "0.1") # allow some time for control valve to open to
desired position
  field(DLY4, "0.01") #
  field(LNK1, "$(SYS):Get-InitP.VAL PP")# Get Initial Position Before
Any Movement was started
  field(LNK2, "$(SYS):$(pdcv).VAL PP")
  field(LNK3, "$(SYS):$(ppr).VAL PP")
  field(LNK4, "$(SYS):Motion-Initiated.VAL PP")
  field(LNK5, "$(SYS):Enable-Timer.PROC PP")
  field(LNK6, "$(SYS):Put-OldD.PROC PP")
  #field(LNK7, "$(SYS):Auto-Reached.PROC PP")
  field(SELM, "All")
}
#####
# Stop Drive : position is reached within 0.1 mm
# of selected position(Put-P.VAL).
# this maybe adjusted to account for pot noise
#####
record(calcout, "$(SYS):Pos-Reached") {
  field(SCAN, "$(scan)")
  field(FLNK, "$(SYS):Auto-Reached")
  #field(CALC, "A&&B&&ABS(C-D)<=$(potNoise)?$(on):$(off)")
  field(CALC, "ABS(C-D)>0&&ABS(C-D)>$(potNoise)?$(on):$(off)")
  field(INPA, "$(SYS):Motion-Started NPP")# user selection
  field(INPB, "$(SYS):Drive-State NPP")# user selection
  field(INPC, "$(SYS):Put-P NPP")# user selection
  field(INPD, "$(SYS):Get-P PP") # Pot readback
  #field(OUT, "$(SYS):Stop-Motion.PROC PP")
  field(OUT, "$(SYS):Stop-Reached.PROC PP")
  field(OOPT, "Transition To Non-zero")
}

record(seq, "$(SYS):Stop-Reached") {
  field(SCAN, "Passive")
  field(DOL1, "$(on)")
  field(DOL2, "$(on)")
  field(DLY2, "0.5") # delay for motor to come to stop
  field(LNK1, "$(SYS):Stop-Motion.PROC PP")
  field(LNK2, "$(SYS):Auto-Reached.PROC PP")
  field(SELM, "All")
}
#####
# We need to confirm that an auto position was reached

```

```

# Put-Auto is on when an auto position is selected
# when a position is reached
#####
record(calc, "$ (SYS):Auto-Reached") {
    field(PINI, "YES")
    field(CALC, "ABS(A-B)<=0.5?$ (on):$ (off)")
    field(INPA, "$ (SYS):Put-P NPP") # user selection
    field(INPB, "$ (SYS):Get-P PP") # Pot readback
}

record(calcout, "$ (SYS):Put-Reached") {
    field(PINI, "YES")
    field(CALC, "A&&B?$ (on):$ (off)")
    field(INPA, "$ (SYS):Put-Auto NPP") # Pot readback
    field(INPB, "$ (SYS):Auto-Reached NPP") # user selection
    #field(OUT, "$ (SYS):Put-Auto PP")
    #field(OOPT, "Transition To Zero")
}

#####
# Emergency Checks
# 1. Check that Motion was started
# 2. Start a count timer
# 3. Check State : idle or In motion : subtract Get-P from Put-P
# if idling(<< 1mm) thus initiate cold start operation otherwise do
nothing
# Init Timer only after Motion was initiated: disable it after timeout
#####
record(scalcout, "$ (SYS):Enable-Timer") {
    field(DTYP, "Soft Channel")
    field(PINI, "YES")
    field(INPA, "$ (SYS):Motion-Initiated")
    field(CALC, "A?AA:BB")
    field(AA, "$ (startTimer)") #0
    field(BB, "$ (stopTimer)") #1
    field(OUT, "$ (SYS):EmStart-TimeOut.SCAN PP")
}

#####
# Counter Routine
#####
record(calcout, "$ (SYS):EmStart-TimeOut") {
    field(SCAN, "Passive")
    #field(PINI, "YES")
    field(CALC, "A<=0?$ (on):$ (off)")
    field(INPA, "$ (SYS):EmStart-Counter PP")
    field(OUT, "$ (SYS):Reset-Timer PP")
    field(OOPT, "Transition To Non-zero")
}

record(calc, "$ (SYS):EmStart-Counter") {
    field(SCAN, "Passive")
    field(CALC, "B&&A>=0?A-1:$ (emStartCnt)")
    field(INPA, "$ (SYS):EmStart-Counter NPP")
    field(INPB, "$ (SYS):Motion-Initiated NPP")
    field(VAL, "$ (emStartCnt)")
}

#####

```

```

# Time Out: reset Motion initiated flag
# check for ~5 mm displacement
#####
record(seq, "$(SYS):Reset-Timer") {
  field(SCAN, "Passive")
  field(DOL1,"$(off)")
  field(DOL2,"$(on)")
  field(DOL3,"$(on)")
  field(DOL4,"$(off)")
  field(DLY2, "0.1") #
  field(LNK1, "$(SYS):Motion-Initiated PP")
  field(LNK2, "$(SYS):Enable-Timer.PROC PP")
  field(LNK3, "$(SYS):Check-Motion.PROC PP")
  field(SELM, "All")
}
#####
####
# return lnk1 if motion started
# return lnk2 otherwise
#####
###
record(calc, "$(SYS):Check-Motion") {
  field(SCAN, "Passive")
  field(FLNK,"$(SYS):Drive-Status")
  field(CALC, "ABS(A-B)>=$(emMinDisp)?$(lnk1):$(lnk2) ")
  field(INPA, "$(SYS):Get-InitP NPP")
  field(INPB, "$(SYS):Get-P PP")
}
#####
record(seq, "$(SYS):Drive-Status") {
  field(SCAN, "Passive")
  field(DOL1,"$(on)")
  field(DOL2,"$(on)")
  field(LNK1, "$(SYS):Motion-Act.PROC PP")
  field(LNK2, "$(SYS):EmStart-Act.VAL PP")
  field(SELM, "Specified")
  field(SELL, "$(SYS):Check-Motion")
}

record(seq, "$(SYS):Motion-Act") {
  field(SCAN, "Passive")
  field(DOL1,"$(off)")
  field(DOL2,"$(on)")
  field(DOL3,"$(on)")
  field(DOL4,"$(off)")
  field(LNK1, "$(SYS):Motion-Initiated PP")
  field(LNK2, "$(SYS):Motion-Started PP")
  field(LNK3, "$(SYS):Drive-State PP")
  field(LNK4, "$(SYS):EmStart-Act.VAL PP")
  field(SELM, "All")
}
#####
## Control Motion
## Secure Carousel: Implement hard limits
#####
record(calcout, "$(SYS):HardLmt-Act") {
  field(SCAN, "$(scan)")
  field(PINI, "YES")
}

```

```

    field(CALC, "A||B?$(on):$(off)")
    field(INPA, "$(SYS):$(limIn) NPP")
    field(INPB, "$(SYS):$(limOut) NPP")
    field(OUT, "$(SYS):Stop-Motion.PROC PP")
    field(OOPT, "Transition To Non-zero")
}
#####
## Control Motion
## Secure Carousel: Implement soft limits
## Soft Limit In is engaged beyond alignment of Bottom target
## Soft Limit Out is engaged beyond alignment of Top target
#####
record(calcout, "$(SYS):SoftLmt-In") {
    field(SCAN, "$(scan)")
    field(PINI, "YES")
    field(FLNK, "$(SYS):LmtIn-Act")
    field(CALC, "A&&B>=C?$(on):$(off)")
    field(INPA, "$(SYS):SoftLmt-Act NPP") # operator activate soft limit
here
    field(INPB, "$(SYS):Get-P PP")
    field(INPC, "$(softLmtIn)")
    field(OUT, "$(SYS):Stop-Motion.PROC PP")
    field(OOPT, "Transition To Non-zero")
}

#record(seq, "$(SYS):SoftLmtIn-State") {
#    field(SCAN, "$(scan)")
#    field(FLNK, "$(SYS):LmtIn-Act")
#    field(DOL1, "$(on)")
#    field(DOL2, "$(off)")
#    field(LNK1, "$(SYS):Stop-SoftLmtIn.PROC PP")
#    field(LNK2, "$(SYS):SoftLmtIn-On.VAL PP")
#    field(SELM, "Specified")
#    field(SELL, "$(SYS):SoftLmt-In PP")
#}

#record(seq, "$(SYS):Stop-SoftLmtIn") {
#    field(SCAN, "Passive")
#    field(DOL1, "$(on)")
#    field(DOL2, "$(on)")
#    field(LNK1, "$(SYS):Stop-Motion.PROC PP")
#    field(LNK2, "$(SYS):SoftLmtIn-On.VAL PP")
#    field(SELM, "All")
#}
#####
#####
record(calcout, "$(SYS):SoftLmt-Out") {
    field(SCAN, "$(scan)")
    field(PINI, "YES")
    field(FLNK, "$(SYS):LmtOut-Act")
    field(CALC, "A&&B<=C?$(on):$(off)")
    field(INPA, "$(SYS):SoftLmt-Act NPP") # operator activate soft limit
here
    field(INPB, "$(SYS):Get-P PP")
    field(INPC, "$(softLmtOut)")
    field(OUT, "$(SYS):Stop-Motion.PROC PP")
    field(OOPT, "Transition To Non-zero")
}

```



```

#record(seq, "$(SYS):SoftLmtOut-State") {
# field(SCAN, "$(scan)")
# field(DOL1, "$(on)")
# field(DOL2, "$(off)")
# field(FLNK, "$(SYS):LmtOut-Act")
# field(LNK1, "$(SYS):Stop-SoftLmtOut.PROC PP")
# field(LNK2, "$(SYS):SoftLmtOut-On.VAL PP")
# field(SELM, "Specified")
# field(SELL, "$(SYS):SoftLmt-Out PP")
#}

#record(seq, "$(SYS):Stop-SoftLmtOut") {
# field(SCAN, "Passive")
# field(DOL1, "$(on)")
# field(DOL2, "$(on)")
# field(LNK1, "$(SYS):Stop-Motion.PROC PP")
# field(LNK2, "$(SYS):SoftLmtOut-On.VAL PP")
# field(SELM, "All")
#}
#####
### Control Motion: Update Display with status
#####
record(calc, "$(SYS):LmtIn-Act") {
    field(PINI, "YES")
    field(CALC, "A|B?$(on):$(off)")
    field(INPA, "$(SYS):$(limIn) NPP")
    field(INPB, "$(SYS):SoftLmtIn-On.VAL PP")
}
record(calc, "$(SYS):LmtOut-Act") {
    field(PINI, "YES")
    field(CALC, "A|B?$(on):$(off)")
    field(INPA, "$(SYS):$(limOut) NPP")
    field(INPB, "$(SYS):SoftLmtOut-On.VAL PP")
}
#####
# Limit status and flags
#####
record(bo, "$(SYS):SoftLmt-Act") {
    field(SCAN, "Passive")
    field(PINI, "YES")
    field(ZNAM, "OFF")
    field(ONAM, "ON")
    field(VAL, "1")
}
record(bo, "$(SYS):SoftLmtIn-On") {
    field(SCAN, "Passive")
    field(OMSL, "closed_loop")
    field(DOL, "$(SYS):SoftLmt-In.VAL NPP")
    field(PINI, "YES")
    field(ZNAM, "OFF")
    field(ONAM, "ON")
    field(VAL, "0")
}
record(bo, "$(SYS):SoftLmtOut-On") {
    field(SCAN, "Passive")
    field(OMSL, "closed_loop")
    field(DOL, "$(SYS):SoftLmt-Out.VAL NPP")
}

```

```

    field(PINI, "YES")
    field(ZNAM, "OFF")
    field(ONAM, "ON")
    field(VAL, "0")
}
#####
# Control Motion: Emergency Stop
#####
record(bo, "$(SYS):Em-Stop") {
    field(SCAN, "Passive")
    field(FLNK, "$(SYS):Put-EmStop")
    field(PINI, "YES")
    field(ZNAM, "OFF")
    field(ONAM, "ON")
    field(VAL, "0")
}
record(calcout, "$(SYS):Put-EmStop") {
    field(SCAN, "Passive")
    field(CALC, "A?$(on):$(off)")
    field(INPA, "$(SYS):Em-Stop NPP")
    field(OUT, "$(SYS):Stop-Motion.PROC PP")
    field(OOPT, "Transition To Non-zero")
}
#####
### Control Motion: Abort Manual move
#####
#record(calcout, "$(SYS):Abort-Stop") {
# field(SCAN, "Passive")
# field(PINI, "YES")
# field(CALC,
"A!=$(topCnts) &&A=!$(midCnts) &&A=!$(botCnts) &&B?$(on):$(off)")
# field(INPA, "$(SYS):Put-P NPP")
# field(INPB, "$(SYS):Put-Abort NPP")

# field(OUT, "$(SYS):Stop-Motion.PROC PP")
# field(OOPT, "Transition To Non-zero")
#}
#####
# Stop Motion by closing all valves
# maybe need to update this record after motor is tested for stop
# Init this record to reset all drive parameters
#####
record(seq, "$(SYS):Stop-Motion") {
    field(SCAN, "Passive")
    field(PINI, "YES")
    field(DOL1, "$(pdcvOff)")
    field(DOL2, "$(pprOff)")
    field(DOL3, "$(off)")
    field(DOL4, "$(off)")
    field(DOL5, "$(off)")
    field(DOL6, "$(off)")
    field(DOL7, "$(off)")
    field(DOL8, "$(on)")
    field(DOL9, "$(on)")
    field(DOLA, "$(on)")
    field(DLY2, "0.5") # allow some time for control valve to open to
desired position

```

```

field(DLY4, "0.1") # allow some time for for drive to stop
field(LNK1, "$(SYS):$(pdcv) PP")
field(LNK2, "$(SYS):$(ppr) PP")
field(LNK3, "$(SYS):Motion-Initiated.VAL PP")
# Ensure that the init value in put-P does not initiate movement
field(LNK4, "$(SYS):P-Selected PP")
field(LNK5, "$(SYS):Drive-State.VAL PP")
field(LNK6, "$(SYS):Motion-Started.VAL PP")
field(LNK7, "$(SYS):EmStart-Act.VAL PP")
field(LNK8, "$(SYS):Enable-Timer.PROC PP")
field(LNK9, "$(SYS):Auto-Reached.PROC PP")
field(LNKA, "$(SYS):Put-OldD.PROC PP")
field(SELM, "All")
}

#####
# Origination
#####
record(bo, "$(SYS):Put-Org") {
    field(SCAN, "Passive")
    field(PINI, "YES")
    field(ZNAM, "OFF")
    field(ONAM, "ON")
    field(VAL, "0")
}

#####
# Abort Manual Move
#####
record(bo, "$(SYS):Put-Abort") {
    field(SCAN, "Passive")
    field(PINI, "YES")
    field(ZNAM, "OFF")
    field(ONAM, "ON")
    field(VAL, "0")
}

#####
# Emergency start sequence
#####
record(bo, "$(SYS):Em-Start") {
    field(SCAN, "Passive")
    field(PINI, "YES")
    field(ZNAM, "OFF")
    field(ONAM, "ON")
    field(VAL, "0")
}

record(bo, "$(SYS):EmStart-Act") {
    field(SCAN, "Passive")
    field(PINI, "YES")
    field(ZNAM, "OFF")
    field(ONAM, "ON")
    field(VAL, "0")
}

#####
# Flag to indicate that a position was selected
#####
record(bo, "$(SYS):P-Selected") {
    field(PINI, "YES")
    field(ZNAM, "OFF")
}

```

```

    field(ONAM, "ON")
    field(VAL, "0")
}
#####
# Flag to indicated that Motion sequence was started
#####
record (bo, "$(SYS):Motion-Started") {
    field(PINI, "YES")
    field(ZNAM, "OFF")
    field(ONAM, "ON")
    field(VAL, "0")
}

record (bo, "$(SYS):Motion-Initiated") {
    field(PINI, "YES")
    field(ZNAM, "OFF")
    field(ONAM, "ON")
    field(VAL, "0")
}

record (bo, "$(SYS):P-Reached") {
    field(PINI, "YES")
    field(ZNAM, "OFF")
    field(ONAM, "ON")
    field(VAL, "0")
}

record (bo, "$(SYS):Put-Auto") {
    field(PINI, "YES")
    field(ZNAM, "OFF")
    field(ONAM, "ON")
    field(VAL, "0")
}
#####
# Dirve is either in Motion or Idling
#####
record(bo, "$(SYS):Drive-State") {
    field(SCAN, "Passive")
    field(PINI, "YES")
    field(ZNAM, "Idle")
    field(ONAM, "In Motion")
    field(VAL, "0")
}

record (bo, "$(SYS):Soft-IntlksError") {
    field(PINI, "YES")
    field(ZNAM, "OFF")
    field(ONAM, "ON")
    field(VAL, "0")
}
#####
# These are for simulation purposes
#####
#record (calcout, "$(SYS):EtherCAT-Interlocks") {
#    field(PINI, "YES")
#    field(CALC, "0")
#}
#record (ao, "$(SYS):PPRSETP:RAW") {
#}

```

```
#record (ao, "$(SYS):PDCVSETP:RAW") {
#}
#record (bo, "$(SYS):CL1LIM-IN") {
#}
#record (bo, "$(SYS):CL1LIM-OUT") {
#}
#record(ao,"$(SYS):Get-P")
#{
# field(DTYP,"Soft Channel")
# field(VAL, "$(topMm)")
# field(PINI,"YES")
# field(HOPR, "$(mmMax)")
# field(LOPR, "$(mmMin)")
#}
```